J. Fluid Mech. (1999), *vol.* 388, *pp.* 115–145. Printed in the United Kingdom

Planetary waves in a stratified ocean of variable depth. Part 1. Two-layer model

By G. M. REZNIK AND T. B. TSYBANEVA

P. P. Shirshov Institute of Oceanology, Russian Academy of Sciences, Krasikova, 23, Moscow 117218, Russia

(Received 22 July 1996 and in revised form 15 December 1998)

Linear Rossby waves in a two-layer ocean with a corrugated bottom relief (the isobaths are straight parallel lines) are investigated. The case of a rough bottom relief (the wave scale L is much greater than the bottom relief scale L_b) is studied analytically by the method of multiple scales. A special numerical technique is developed to investigate the waves over a periodic bottom relief for arbitrary relationships between L and L_b.

There are three types of modes in the two-layer case: barotropic, topographic, and baroclinic. The structure and frequencies of the modes depend substantially on the ratio $\Delta = (\Delta h/h_2)/(L/a)$ measuring the relative strength of the topography and β-effect. Here $\Delta h/h_2$ is the typical relative height of topographic inhomogeneity and a is the Earth's radius. The topographic and barotropic mode frequencies depend weakly on the stratification for small and large Δ and increase monotonically with increasing Δ. Both these modes become close to pure topographic modes for $\Delta \gg 1$.

The dependence of the baroclinic mode on Δ is more non-trivial. The frequency of this mode is of the order of $f_0 L_i^2/aL$ (L_i is the internal Rossby scale) irrespective of the magnitude of Δ. At the same time the spatial structure of the mode depends strongly on Δ. With increasing Δ the relative magnitude of motion in the lower layer decreases. For $\Delta \gg 1$ the motion in the mode is confined mainly to the upper layer and is very weak in the lower one. A similar concentration of mesoscale motion in an upper layer over an abrupt bottom topography has been observed in the real ocean many times.

Another important physical effect is the so-called 'screening'. It implies that for $L_b < L_i$ the small-scale component of the wave with scale L_b is confined to the lower layer, whereas in the upper layer the scale of the motion L is always greater than or of the order of, L_i. In other words, the stratification prevents the ingress of motion with scale smaller than the internal Rossby scale into the main thermocline.

1. Introduction

The bottom relief along with the β-effect plays a key role in the dynamics of mesoscale motion in the ocean. The effect of topography is determined by the bottom boundary condition, which can be written as

$$w = u\frac{\partial h}{\partial x} + v\frac{\partial h}{\partial y}, \quad z = h(x, y). \tag{1.1}$$

Here x, y, and z are the eastward, northward, and vertical coordinates, respectively; u, v, and w are the zonal, meridional, and vertical velocity components; and $h = h(x, y)$ is the variable oceanic depth. By virtue of (1.1), the typical value of the near-bottom

vertical velocity generated by the flow interaction with an uneven bottom is

$$W_b = U_n \frac{\Delta h}{L_b}, \tag{1.2}$$

where U_n is the typical velocity component normal to the isobathes and Δh and L_b are the characteristic height and horizontal scale of the bottom inhomogeneities, respectively. Another limitation on the vertical velocity follows from the equation for the vertical vorticity component $\Omega = (\partial v/\partial x) - (\partial u/\partial y)$ (Pedlosky 1979):

$$\frac{\partial \Omega}{\partial t} + u\frac{\partial \Omega}{\partial x} + v\frac{\partial \Omega}{\partial y} - f_0 \frac{\partial w}{\partial z} + \beta v = 0, \tag{1.3}$$

where t is time and $f = f_0 + \beta y$ the Coriolis parameter. It is easy to see from (1.3) that the vertical velocity scale W satisfies the condition

$$W \lesssim \max(\varepsilon_T, Ro, \varepsilon_R)\frac{H}{L}U. \tag{1.4}$$

Here $\varepsilon_T = (Tf_0)^{-1}$; Ro is the Rossby number, $Ro = U/f_0 L$; U is the horizontal velocity scale; $\varepsilon = L/a$; and a is the Earth's radius.

Here we are interested in the mesoscale quasi-geostrophic motion for which the parameters ε_T, Ro, and ε_R, are small as compared to unity:

$$\varepsilon_T \ll 1, \quad Ro \ll 1, \quad \varepsilon_R \ll 1, \tag{1.5}$$

and the vertical scale H is of the order of the oceanic depth and is much smaller than the horizontal scale L:

$$\frac{H}{L} \ll 1. \tag{1.6}$$

Because W_b cannot exceed W, (1.2) and (1.4) imply

$$\frac{U_n}{U} \lesssim \max(\varepsilon_T, Ro, \varepsilon_R)\frac{H}{\Delta h}\frac{L_b}{L}. \tag{1.7}$$

Let the relative height $\Delta h/H$ of the bottom bumps be sufficiently small so that

$$\frac{\Delta h}{H} \lesssim \max(\varepsilon_T, Ro, \varepsilon_R)\frac{L_b}{L}. \tag{1.8a}$$

Under condition (1.8a) the right-hand side of (1.7) is of the order of or greater than unity, i.e. the velocity components across and along the isobaths can be of the same order, and the fluid particles move freely across the isobaths. On the other hand, if $\Delta h/H$ is sufficiently large, i.e.

$$\frac{\Delta h}{H} \gg \max(\varepsilon_T, Ro, \varepsilon_R)\frac{L_b}{L}, \tag{1.8b}$$

then the right-hand side of (1.7) is smaller than unity and the near-bottom flow is directed approximately along the isobaths. The cases (1.8a) and (1.8b) will be referred to as the moderate and strong topography, respectively.

Conditions (1.7), (1.8a, b) essentially depend on the relationship between the topography scale L_b and the motion scale L. In the case of smooth bottom topography, $L \ll L_b$, condition (1.8a) can be rewritten in the form

$$\frac{\Delta h}{L_b} L \leqslant \max(\varepsilon_T, Ro, \varepsilon_R)H. \tag{1.9}$$

Inequality (1.9) means that the characteristic depth difference across the scale of

motion $(\Delta h/L_b)L$ must be sufficiently small compared to the fluid depth H for the fluid particles to be able to move across the slope. If the bottom topography is undulatory, i.e. $L \sim L_b$, then conditions (1.7) and (1.8a, b) reduce to

$$\frac{U_n}{U} \lesssim \max(\varepsilon_T, Ro, \varepsilon_R)\frac{H}{\Delta h}, \tag{1.10}$$

$$\frac{\Delta h}{H} \lesssim \max(\varepsilon_T, Ro, \varepsilon_R), \tag{1.11a}$$

$$\frac{\Delta h}{H} \gg \max(\varepsilon_T, Ro, \varepsilon_R). \tag{1.11b}$$

In the case of a rough bottom, $L \gg L_b$, the motion can be considered as a superposition of a large-scale component with scale L and a small-scale one with topography scale L_b. (The classification of bottom topography depending on the relationship between the scales L and L_b was introduced by Rhines & Bretherton (1973)). For example, the velocity field is represented as follows:

$$\boldsymbol{U} = \boldsymbol{U}_L\left(\frac{x}{L}, \frac{y}{L}, \frac{z}{H}, t\right) + \boldsymbol{U}_s\left(\frac{x}{L_b}, \frac{y}{L_b}, \frac{x}{L}, \frac{y}{L}, \frac{z}{H}, t\right). \tag{1.12}$$

Here $\boldsymbol{U}_L$ and $\boldsymbol{U}_s$ are the large- and small-scale parts. The relationship between them is not known *á priori*, but one can suppose that the small-scale bottom relief is dynamically important if

$$U_s \gtrsim U_L \tag{1.13}$$

in at least the near-bottom region. Using (1.13) and the inequality $L \gg L_b$ one can readily prove the applicability of conditions (1.10) and (1.11a, b) for the case of a rough bottom.

There is a significant distinction between the barotropic and baroclinic flows over a strong topography. In accordance with the Taylor–Proudman theorem, the barotropic fluid moves approximately along the isobaths from top to bottom. In a stratified ocean this theorem is inapplicable, and therefore the regime is possible when the strong topography forces the near-bottom fluid to flow along the isobaths but affects weakly the upper fluid motion. In other words, the stratification is capable of 'isolating' the upper layer motion from the influence of the strong topography which dominates the abyssal dynamics. We believe that this screening is realized in the real ocean because no substantial correlation between the underlying topography and the horizontal structure of the upper layer mesoscale motion was observed even in the regions with very strong bottom topography. At the same time, the vertical structure of mesoscale motion is strongly affected by the bottom relief (Wunsch 1981, 1983; Dickson 1983). The motion over the abrupt topography is very weak in the abyssal region and is confined predominantly to the main thermocline. Rhines (1977) revealed an analogous effect in numerical experiments with a two-layer model. Obviously, this vertical structure can exist only due to stratification.

The existing theory of mesoscale quasigeostrophic motion usually restricts the consideration to the moderate topography case (1.8a) (Pedlosky 1979; Kamenkovich, Koshlyakov & Monin 1986). However, the quasigeostrophic approximation means only the smallness of the parameters ε_T, Ro, and ε_R and imposes no constraints on the bottom relief.

The primary aim of the present paper is to investigate the joint effect of stratification and bottom topography, both moderate and strong, on the quasigeostrophic oceanic

motion. This is a complicated problem, and we restrict our consideration to the low-frequency quasi-geostrophic modes over one-dimensional bottom topography (the isobaths are parallel straight lines). The simplest case of uniformly sloping bottom was investigated by Rhines (1970). He has found that two types of modes exist over a sufficiently steep slope: the faster bottom-trapped mode and the slower mode isolated from the bottom (with almost zero velocity at the bottom). The oscillations over a corrugated bottom topography were considered in the pioneering work by Rhines & Bretherton (1973), who investigated the propagation of barotropic quasi-geostrophic oscillations over a bottom relief of this kind. The most important result of their work is that rough corrugated relief supports propagating waves with $L > L_b$ even in the absence of β-effect. Volosov (1976*a*, *b*) modified this theory taking into account nonlinear effects. The stratified case was investigated by Suarez 1971; McWilliams 1974; Volosov & Zhdanov 1980*a*, *b*, 1982, 1983; and Zhdanov 1987. Finally, the case of random corrugated relief in the barotropic ocean was analysed by Sengupta, Piterbarg & Reznik (1992).

All these works (except the last one) use the following constraints on the wave parameters:

$$\varepsilon_R \lesssim \varepsilon_T \sim \frac{\Delta h}{H} \sim \frac{L_b}{L} \ll 1, \tag{1.14}$$

where $\varepsilon_T = \sigma/f_0$ and σ is the wave frequency. Clearly, relations (1.14) imply the condition (1.11*a*) for moderate topography.

The case of a strong corrugated relief was also considered in a number of papers. Samelson (1992, 1998) performed a numerical analysis of the eigenmodes in a two-layer ocean with sinusoidal undulating bottom topography. The main result of his work is the existence of a surface-intensified Rossby mode with frequency exceeding the flat-bottom baroclinic cut-off frequency. Reznik (1986) showed that an analogous mode occurs over a rough-bottom topography. The condition (1.11*b*) for strong topography holds for the surface-intensified baroclinic modes.

In the present work we investigate low-frequency quasi-geostrophic oscillations in a two-layer ocean with undulating or rough bottom topography for more general relations among the parameters ε_R, ε_T, $\Delta h/H$, and L_b/L than (1.14). Particular attention will be given to the case of strong topography where the parameters satisfy (1.11*b*).

In § 2 the model under consideration is described. After that an asymptotic theory of Rossby waves over a rough bottom topography is developed (§§ 3, 4). In § 5 the baroclinic modes over a strong periodic rough relief are investigated. Waves over an arbitrary periodic relief are considered in § 6. Conclusions are stated in § 7.

2. Statement of the problem

Large-scale low-frequency oscillations with time scales of the order of several days and larger and space scales from tens to hundreds of kilometres are governed by the well-known equation of conservation of potential vorticity; in the case of a two-layer ocean on the β-plane in the linear and rigid-lid approximations we have

$$\frac{\partial}{\partial t}\left[\Delta\Psi_1 - \alpha_1 L_i^{-2}(\Psi_1 - \Psi_2)\right] + \beta\frac{\partial \Psi_1}{\partial x} = 0, \tag{2.1a}$$

$$\frac{\partial}{\partial t}\left[\Delta\Psi_2 + \alpha_2 L_i^{-2}(\Psi_1 - \Psi_2)\right] + \beta\frac{\partial \Psi_2}{\partial x} + \frac{f_0}{h_2}J(\Psi_2, b) = 0. \tag{2.1b}$$

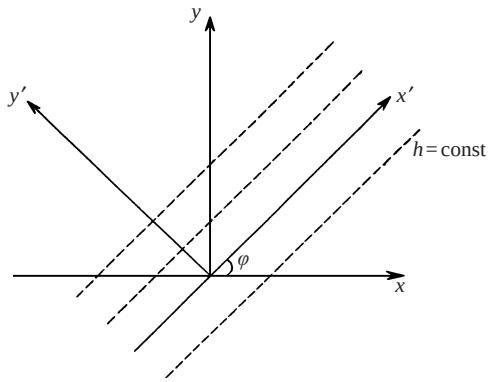

FIGURE 1. Isobaths (dashed lines) and coordinates.

Here Ψ_k, h_k, $k = 1, 2$ are the streamfunctions and constant mean depths of the layers, respectively; the subscripts 1 and 2 correspond to the upper and lower layers, respectively; $\alpha_1 = h_2/(h_1 + h_2)$ and $\alpha_2 = h_1/(h_1 + h_2)$; $L_i = (g'h_1h_2)^{1/2}/(f_0^2(h_1 + h_2))^{1/2}$ is the internal Rossby scale; $g' = g\Delta\rho/\rho_0$ is the reduced gravitational acceleration; ρ_0 is the mean density, $\Delta\rho = \rho_2 - \rho_1$; $h_{2t} = h_2 + b(x, y)$ is the lower layer depth; and b, $b \ll h_2$, is the depth perturbation.

Let the bottom topography be corrugated, i.e.

$$b = b(-x\sin\varphi + y\cos\varphi), \tag{2.2}$$

where φ is a constant angle between the isobaths and the zonal direction (figure 1). We now rewrite (2.1*a*, *b*) in the coordinates x', y' directed along and across the isobaths, respectively (see figure 1):

$$x' = x\cos\varphi + y\sin\varphi, \tag{2.3a}$$

$$y' = -x\sin\varphi + y\cos\varphi. \tag{2.3b}$$

Omitting the primes we have

$$\frac{\partial}{\partial t}\left[\Delta\Psi_1 - \alpha_1 L_i^{-2}(\Psi_1 - \Psi_2)\right] + \beta\left(\frac{\partial\Psi_1}{\partial x}\cos\varphi - \frac{\partial\Psi_1}{\partial y}\sin\varphi\right) = 0, \tag{2.4a}$$

$$\frac{\partial}{\partial t}\left[\Delta\Psi_2 + \alpha_2 L_i^{-2}(\Psi_1 - \Psi_2)\right] + \beta\left(\frac{\partial\Psi_2}{\partial x}\cos\varphi - \frac{\partial\Psi_2}{\partial y}\sin\varphi\right) + \frac{f_0}{h_2}\frac{\partial b}{\partial y}\frac{\partial\Psi_2}{\partial x} = 0. \tag{2.4b}$$

Let the motion depend harmonically on x and t, i.e.

$$\Psi_n = \psi_n(y)\exp\left[\mathrm{i}(kx - \sigma t)\right], \quad n = 1, 2, \tag{2.5}$$

and let the seafloor perturbation have the form

$$b = \Delta h\hat{b}(\hat{y}), \tag{2.6}$$

where Δh is the characteristic value of depth fluctuations and $\hat{b}$ is the non-dimensional function of the coordinate $\hat{y} = y/L_b$. On representing Ψ_k in the form (2.5) in (2.4*a*, *b*) and writing the resulting equations in non-dimensional form with L_b as lengthscale we obtain the equations

$$\psi_1'' - \frac{\mathrm{i}\hat{\beta}}{\hat{\sigma}}\psi_1'\sin\varphi - \left(\hat{k}^2 + \alpha_1 q + \frac{\hat{\beta}\hat{k}}{\hat{\sigma}}\cos\varphi\right)\psi_1 + \alpha_1 q\psi_2 = 0, \tag{2.7a}$$

$$\psi_2'' - \frac{\mathrm{i}\hat{\beta}}{\hat{\sigma}}\psi_2' \sin\varphi - \left(\hat{k}^2 + \alpha_2 q + \frac{\hat{\beta}\hat{k}}{\hat{\sigma}}\cos\varphi + \frac{\hat{k}\delta}{\hat{\sigma}}\hat{b}'\right)\psi_2 + \alpha_2 q\psi_1 = 0. \tag{2.7b}$$

Here

$$\hat{k} = kL_b, \quad \hat{\sigma} = \sigma/f_0, \quad \delta = \Delta h/h_2, \quad q = L_b^2/L_i^2, \quad \hat{\beta} = \beta L_b/f_0, \tag{2.8}$$

and the prime denotes differentiation with respect to $\hat{y}$. The parameters (2.8) are not arbitrary, but satisfy some conditions. We consider quasi-geostrophic motion, and therefore the parameter $\hat{\sigma} = \sigma/f_0$ is small:

$$\hat{\sigma} = \sigma/f_0 \ll 1. \tag{2.9a}$$

The scale L_b is assumed to be no greater than 50 km, and therefore

$$\hat{\beta} \simeq L_b/a = O(0.01), \tag{2.9b}$$

$$q \lesssim 1. \tag{2.9c}$$

At the same time, we assume that the typical height Δh is much smaller than the lower depth h_2, i.e.

$$\delta = \frac{\Delta h}{h_2} \ll 1. \tag{2.9d}$$

We also have

$$\hat{k} = kL_b = \frac{L_b}{L} \lesssim 1 \tag{2.9e}$$

because we are interested in either undulating or rough relief cases.

Our task is to investigate the eigenvalue problem (2.7a, b), i.e. given δ, q, and $\hat{\beta}$, to find the eigenvalues $\hat{k}$ and $\hat{\sigma}$ providing the existence of bounded solutions to (2.7a, b) and to study the properties of the eigenfunctions.

The conditions of moderate and strong topography (1.11a, b) are written in terms of the parameters δ, $\hat{\sigma}$, $\hat{\beta}$, $\hat{k}$ as follows:

$$\delta \lesssim \max(\hat{\sigma}, \hat{\beta}/\hat{k}), \tag{2.10a}$$

$$\delta \gg \max(\hat{\sigma}, \hat{\beta}/\hat{k}). \tag{2.10b}$$

To simplify the notation, in what follows we drop the hat over the non-dimensional parameters $\hat{k}$, $\hat{\sigma}$, $\hat{\beta}$, $\hat{y}$, and $\hat{b}$.

3. Heuristic asymptotic theory for rough relief

In the general case the eigenvalue problem (2.7a, b) is complicated, but some analytical progress is possible for the rough relief when

$$k \ll 1 \tag{3.1}$$

(also see Reznik 1986). There are four small parameters k, σ, δ, and β, and the uncertain parameter q in (2.7a, b). In such a situation it is common practice to prescribe some relations between small parameters to express all the parameters in terms of one of them (as in the works by Rhines & Bretherton and Volosov & Zhdanov cited above). However, in reality, the parameters k, σ, δ, and β are independent and vary over a wide range, and therefore we choose an alternative analysis method for problem (2.7a, b), which is a modification of the method of multiscale asymptotic expansions.

The solution is sought in the form

$$\psi_n = \bar{\psi}_n(Y) + \tilde{\psi}_n(y, Y), \quad n = 1, 2, \tag{3.2}$$

where $Y = ky$ is a slow coordinate. The term $\bar{\psi}_n(Y)$ in (3.2) describes a large-scale wave component and $\tilde{\psi}_n(y, Y)$ represents the small-scale component generated by the interaction of the large-scale component with the rough relief. The small-scale component $\tilde{\psi}_n$ is assumed to satisfy two additional conditions: (i) the mean values of $\tilde{\psi}_n$ are zero, i.e.

$$\langle \tilde{\psi}_n \rangle = 0; \tag{3.3}$$

and (ii) the components $\bar{\psi}_n(Y)$ and $\tilde{\psi}_n(y, Y)$ are 'smooth' functions of y, Y. The averaging in (3.3) is carried out with respect to the fast coordinate y:

$$\langle a \rangle = \lim_{L_0 \to \infty} \frac{1}{2L_0} \int_{-L_0}^{L_0} a \, \mathrm{d}y, \tag{3.4}$$

and the smoothness of the function $f(y, Y)$ means that its derivatives with respect to y and/or Y are of the order of the function itself, i.e.

$$\frac{\partial^{m+n} f}{\partial y^m \partial Y^n} = O(f), \quad m = 0, 1, 2, \ldots, \quad n = 0, 1, 2, \ldots \tag{3.5}$$

irrespective of the relationships among k, σ, δ, q, and β.

The depth perturbation $b(y)$ is assumed to be represented as a superposition of a finite number of harmonics in the form

$$b = \sum_{m=-M}^{M} b_m \, \mathrm{e}^{\mathrm{i}l_m y}, \tag{3.6}$$

where $|l_m| \gtrsim 1$, $l_m = -l_{-m}$, and $b_m = b^*_{-m}$ (the asterisk denotes the complex conjugate).

Substituting (3.2) into (2.7a, b), averaging the resulting equations with respect to y, and using (3.3) we derive

$$k^2 \bar{\psi}_{1YY} - \mathrm{i}\frac{\beta k}{\sigma} \bar{\psi}_{1Y} \sin\varphi - \left(k^2 + \alpha_1 q + \frac{\beta k}{\sigma} \cos\varphi \right) \bar{\psi}_1 + \alpha_1 q \bar{\psi}_2 = 0, \tag{3.7a}$$

$$k^2 \bar{\psi}_{2YY} - \mathrm{i}\frac{\beta k}{\sigma} \bar{\psi}_{2Y} \sin\varphi - \left(k^2 + \alpha_2 q + \frac{\beta k}{\sigma} \cos\varphi \right) \bar{\psi}_2 + \alpha_2 q \bar{\psi}_1 - \frac{k\delta}{\sigma} \langle b' \tilde{\psi}_2 \rangle = 0. \tag{3.7b}$$

The subtraction of (3.7a, b) from (2.7a, b) gives

$$\tilde{\psi}_{1yy} + 2k\tilde{\psi}_{1yY} + k^2 \tilde{\psi}_{1YY} - \mathrm{i}\frac{\beta}{\sigma}(\tilde{\psi}_{1y} + k\tilde{\psi}_{1Y}) \sin\varphi - \left(k^2 + \alpha_1 q + \frac{\beta k}{\sigma} \cos\varphi \right) \tilde{\psi}_1 + \alpha_1 q \tilde{\psi}_2 = 0, \tag{3.8a}$$

$$\tilde{\psi}_{2yy} + 2k\tilde{\psi}_{2yY} + k^2 \tilde{\psi}_{2YY} - \mathrm{i}\frac{\beta}{\sigma}(\tilde{\psi}_{2y} + k\tilde{\psi}_{2Y}) \sin\varphi - \left(k^2 + \alpha_2 q + \frac{\beta k}{\sigma} \cos\varphi \right) \tilde{\psi}_2 + \alpha_2 q \tilde{\psi}_1 - \frac{k\delta}{\sigma} \left(b' \tilde{\psi}_2 - \langle b' \tilde{\psi}_2 \rangle + b' \bar{\psi}_2 \right) = 0. \tag{3.8b}$$

The parameter $\beta k/\sigma$ in (3.7a, b) and (3.8a, b) is of the order of $(L_b/a)(f_0/\sigma) \times (L_b/L)$, where σ is the dimensional frequency. For mesoscale motion we have $\sigma/f_0 \gtrsim 0.01$, i.e.

by virtue of (2.9b), $(L_b/a)(f_0/\sigma) = O(1)$. In non-dimensional form we have

$$\frac{\beta}{\sigma} = O(1), \tag{3.9}$$

and (3.1) implies

$$\frac{\beta k}{\sigma} \ll 1. \tag{3.10}$$

We now neglect the small terms in (3.8a, b) taking into account (3.1), (3.10):

$$\tilde{\psi}_{1yy} - \mathrm{i}\frac{\beta}{\sigma}\tilde{\psi}_{1y}\sin\varphi - \alpha_1 q\tilde{\psi}_1 + \alpha_1 q\tilde{\psi}_2 = 0, \tag{3.11a}$$

$$\tilde{\psi}_{2yy} - \mathrm{i}\frac{\beta}{\sigma}\tilde{\psi}_{2y}\sin\varphi - \alpha_2 q\tilde{\psi}_2 + \alpha_2 q\tilde{\psi}_1 - \frac{k\delta}{\sigma}\left(b'\tilde{\psi}_2 - \langle b'\tilde{\psi}_2\rangle\right) = \frac{k\delta}{\sigma}b'\bar{\psi}_2. \tag{3.11b}$$

The coupled systems (3.7) and (3.11) describe the large- and small-scale motion components, respectively.

To solve the problem we introduce the following condition on the wave parameters:

$$d = \frac{k\delta}{\sigma} \ll 1. \tag{3.12}$$

By virtue of (3.12), the last term on the left-hand side of (3.11b) is small compared to $\tilde{\psi}_{2yy}$ and can be neglected. The solution to the corresponding approximate system can be found easily, and after some algebraic transformations it takes the form

$$\tilde{\psi}_n = -\mathrm{i}\frac{k\delta}{\sigma}\bar{\psi}_2 \sum_m \tilde{\psi}_{nm}\mathrm{e}^{\mathrm{i}l_m y}, \quad n = 1, 2, \tag{3.13a}$$

$$\tilde{\psi}_{1m} = \frac{\alpha_1 q b_m}{\left(l_m^2 - (\beta l_m/\sigma)\sin\varphi + q\right)\left(l_m - (\beta/\sigma)\sin\varphi\right)}, \tag{3.13b}$$

$$\tilde{\psi}_{2m} = \frac{\left(l_m^2 - (\beta l_m/\sigma)\sin\varphi + \alpha_1 q\right)b_m}{\left(l_m^2 - (\beta l_m/\sigma)\sin\varphi + q\right)\left(l_m - (\beta/\sigma)\sin\varphi\right)}. \tag{3.13c}$$

Using (3.6) and (3.13c) we calculate the quantities

$$\langle b'\tilde{\psi}_2\rangle = -\frac{k\delta}{\sigma}\bar{\psi}_2 \sum_m d_m|b_m|^2, \tag{3.14a}$$

$$d_m = \frac{\left(l_m^2 + (\beta l_m/\sigma)\sin\varphi + \alpha_1 q\right)l_m}{\left(l_m^2 + (\beta l_m/\sigma)\sin\varphi + q\right)\left(l_m + (\beta/\sigma)\sin\varphi\right)}, \tag{3.14b}$$

and rewrite (3.7b) as follows:

$$k^2\bar{\psi}_{2YY} - \mathrm{i}\frac{\beta k}{\sigma}\bar{\psi}_{2Y}\sin\varphi - \left(k^2 + \alpha_2 q + \frac{\beta k}{\sigma}\cos\varphi - \frac{k^2\delta^2}{\sigma^2}\Sigma\right)\bar{\psi}_2 + \alpha_2 q\bar{\psi}_1 = 0, \tag{3.15a}$$

where the notation

$$\Sigma = \sum_m d_m|b_m|^2 \tag{3.15b}$$

is used. As a result, we have the closed system (3.7a), (3.15a) for determining $\bar{\psi}_1$, and $\bar{\psi}_2$. The solution is sought in the form of a harmonic wave:

$$\bar{\psi}_n = A_n\mathrm{e}^{\mathrm{i}\bar{l}Y}, \quad n = 1, 2, \tag{3.16}$$

where $\bar{l} = O(1)$ and A_n are constant amplitudes.

The equations for the amplitudes A_n have the form

$$\left[\kappa^2 + \alpha_1 q + \frac{\beta}{\sigma}(k\cos\varphi - l\sin\varphi)\right] A_1 - \alpha_1 q A_2 = 0, \tag{3.17a}$$

$$\alpha_2 q A_1 - \left[\kappa^2 + \alpha_2 q + \frac{\beta}{\sigma}(k\cos\varphi - l\sin\varphi) - \frac{k^2\delta^2}{\sigma^2}\Sigma\right] A_2 = 0. \tag{3.17b}$$

Here $l = k\bar{l} \ll 1$ is the large-scale wavenumber along the direction normal to the isobaths and $\boldsymbol{\kappa} = (k, l)$ is the large-scale wave-vector. The solvability condition for (3.17*a*, *b*) gives the dispersion relation

$$\left(\kappa^2 + \frac{\beta k_x}{\sigma} + q - \frac{\delta^2 k^2}{\sigma^2}\Sigma\right)\left(\kappa^2 + \frac{\beta k_x}{\sigma}\right) - \alpha_1 q \frac{\delta^2 k^2}{\sigma^2}\Sigma = 0, \tag{3.18}$$

where $k_x = k\cos\varphi - l\sin\varphi$ is the projection of the wave vector $\boldsymbol{\kappa}$ on the zonal direction.

Note that in the case of zonal bottom relief when $\varphi = 0$ the coefficient d_m in (3.15*b*) is equal to

$$d_m = \frac{l_m^2 + \alpha_1 q}{l_m^2 + q}.$$

For the typical depths h_1 and h_2 equal to 1 km and 4 km, respectively, we have $\alpha_1 = h_2/(h_1 + h_2) = 0.8$. Thus the coefficient d_m is close to unity, and the topographic coefficient $\delta^2\Sigma$ is close to the simple topographic height variance. An analogous situation occurs for non-zonal bottom relief when $\varphi \neq 0$. In this case $\beta/\sigma \ll 1$ for physically interesting modes (see below in this Section) and the coefficient d_m is again close to unity.

Equation (3.18) relates the wave-vector $\boldsymbol{\kappa}$ to the wave frequency σ and describes oscillations over a wide range of parameters β, δ, and q because the only condition for its applicability is the inequality (3.12). We note that for motions satisfying (1.14) we have $\sigma = O(\delta)$, and therefore (3.12) holds in all the above-mentioned papers by Rhines & Bretherton and Volosov & Zhdanov. In the long-wave limit $L \gg L_b \sim L_i$ relation (3.18) coincides with the dispersion relation found by Volosov & Zhdanov (1980*a*), and for $L \sim L_i \gg L_b$ it coincides with the dispersion relation in the paper by Zhdanov (1987).

The structure of oscillations is characterized by the parameters

$$\bar{m} = \frac{|A_2|}{|A_1|}, \quad \tilde{m} = \frac{\{\langle\tilde{\psi}_{2y}^2\rangle\}^{1/2}}{\{\langle\tilde{\psi}_{1y}^2\rangle\}^{1/2}}, \quad r = \frac{\{\langle\tilde{\psi}_{2y}^2\rangle\}^{1/2}}{\kappa|A_2|}. \tag{3.19}$$

The parameter $\bar{m}$ is equal to the ratio of the typical lower and upper layer large-scale velocities, $\tilde{m}$ is equal to the corresponding ratio for the small-scale velocities, and the parameter r characterizes the relation between small- and large-scale components in the lower layer. Using (3.13), (3.17*a*), and (3.9) we obtain

$$\bar{m} = \frac{|\kappa^2 + \beta k_x/\sigma + \alpha_1 q|}{\alpha_1 q}, \tag{3.20a}$$

$$\tilde{m} = O\left[\max\left(1, 1/q\right)\right], \tag{3.20b}$$

$$r = O\left(\frac{k\delta}{\kappa\sigma}\right). \tag{3.20c}$$

By virtue of (3.20b), the ratio $\tilde{m}^{-1}$ of the upper and lower layer small-scale velocities does not exceed the quantity $q = L_b^2/L_i^2$. If $L_b \leqslant 0.3L_i$, then $q \ll 1$, and the small-scale component in the upper layer is much weaker (q^{-1} times) than that in the lower layer. Thus, the stratification 'screens' the upper layer from the penetration of perturbations with scale L_b smaller than the internal Rossby scale L_i.

Obviously, the above method for deriving the approximate solution is not a rigorous asymptotic procedure making it possible to find a solution to an arbitrary accuracy. We only found an approximation of the lowest order that satisfies the equations with a small discrepancy over a wide range of the parameters k, δ, β, and q. To verify this method some special physically reasonable relations among k, δ, β, and σ were analysed. In each case all the parameters were expressed in terms of one of them and the corresponding solution was obtained by the standard averaging method. In all the cases the approximation of the lowest order and the dispersion relation coincide with the above.

4. Oscillation modes

We now consider the dispersion relation (3.18) for some particular cases.

Constant depth

Let the ocean have a constant depth, i.e. let $\delta = 0$ in (3.18). In this case (3.18) has two roots

$$\sigma_1 = \sigma_{bt} = -\frac{\beta k_x}{\kappa^2}, \quad \sigma_2 = \sigma_{bk} = -\frac{\beta k_x}{\kappa^2 + q} \tag{4.1}$$

coinciding, as could be expected, with the frequencies of barotropic (σ_{bt}) and baroclinic (σ_{bk}) Rossby modes in the two-layer ocean of constant depth.

Barotropic case

System (2.1a, b) is transformed to the barotropic potential vorticity equation if $L_i = \infty$, $\Psi_1 = 0$, and Ψ_2 and h_2 are assumed to be the barotropic streamfunction and the oceanic depth, respectively. Accordingly, (3.17a) is satisfied identically and the dispersion relation (3.18) is transformed to the dispersion relation for a barotropic ocean with a corrugated rough bottom relief:

$$\kappa^2 + \frac{\beta k_x}{\sigma} - \frac{\delta^2 k^2}{\sigma^2}\Sigma' = 0, \tag{4.2a}$$

where

$$\Sigma' = \sum_m d'_m |b_m|^2, \quad d'_m = \frac{l_m}{l_m + (\beta/\sigma)\sin\varphi} \tag{4.2b}$$

(Rhines & Bretherton 1973; Kamenkovich & Reznik 1978).

Topographic modes: $\beta = 0$

For $\beta = 0$ (3.18) has two roots

$$\sigma_{1,2} = \pm\frac{k\delta}{\kappa}\left(\frac{\kappa^2 + \alpha_1 q}{\kappa^2 + q}\right)^{1/2} \Sigma^{1/2}. \tag{4.3}$$

For the oceanic case the coefficient $\alpha_1 = h_2/(h_1 + h_2)$ is close to 1 ($\alpha_1 \geqslant 0.75$), and therefore the ratio $(\kappa^2 + \alpha_1 q)/(\kappa^2 + q)$ is also close to 1, and by virtue of (3.14b) and

(4.2*b*) we have $\Sigma \simeq \Sigma'$. It readily follows from (4.2*a*, *b*) and (4.3) that $\sigma_{1,2}$ are close to the frequencies

$$\sigma'_{1,2} = \pm \frac{k\delta}{\kappa} \Sigma'^{1/2} \tag{4.4}$$

of topographic oscillations in a barotropic ocean of depth H_2. Thus, in the absence of β-effect the stratification affects weakly the topographic oscillation frequencies.

The parameters $\bar{m}$ and r are expressed as

$$\bar{m} = 1 + \frac{1}{\alpha_1}\varepsilon, \quad \varepsilon = \kappa^2 q^{-1} = O(L_i^2/L^2), \tag{4.5a}$$

$$r = O(1). \tag{4.5b}$$

By virtue of (4.5*a*), the large-scale component in the lower layer exceeds that in the upper layer, but the ratio of the components depends strongly on the wave scale L. In the long-wave limit $L_i^2/L^2 \ll 1$ the parameter ε is small and $\bar{m} \simeq 1$, i.e. the large-scale component of the long wave is practically barotropic. For $L \simeq L_i$ the parameter $\bar{m}$ differs substantially from 1, and the large-scale velocities in the layers also differ. The relationship (4.5*b*) means that the large- and small-scale components in the lower layer are of the same order.

Zonal isobaths: $\varphi = 0$

In each of the above cases one of the wave-producing factors was omitted (either the bottom relief or the β-effect or the stratification). Consideration of the combined effect of all these factors is simplified for $\varphi = 0$, when the isobaths are parallel to the zonal direction. In this case the coefficients d_m in (3.14*b*) do not depend on the frequency σ and the dispersion relation (3.18) can be reduced to an algebraic cubic equation for σ. It is convenient to rewrite this equation in terms of the variable $\tilde{\sigma} = \sigma/(\beta k/\kappa^2)$:

$$\tilde{\sigma}^3 + p_1\tilde{\sigma}^2 + p_2\tilde{\sigma} - p_3 = 0, \tag{4.6}$$

where

$$p_1 = \frac{1+2\varepsilon}{1+\varepsilon}, \quad p_2 = \frac{\varepsilon}{1+\varepsilon} - \frac{\alpha_1+\varepsilon}{1+\varepsilon}\Delta^2, \quad p_3 = \frac{\varepsilon\Delta^2}{1+\varepsilon},$$

$$\Delta = \frac{k\delta\Sigma^{1/2}/\kappa}{\beta k/\kappa^2}, \quad \varepsilon = \kappa^2 q^{-1} = O\left(\frac{L_i^2}{L^2}\right).$$

The parameter $\tilde{\sigma}$ is equal to the ratio of the wave frequency to the frequency of the barotropic Rossby wave and the parameter $\Delta = O\left[(\Delta h/h_2)/(L/a)\right]$ measures the relative contributions of the topography and β-effect.

Since $\alpha_1 < 1$ the three roots of (4.6) are real. Therefore, contrary to the cases considered above, *three* wave frequencies σ_1, σ_2, and σ_3 correspond to each wave vector $\boldsymbol{\kappa} = (k, l)$. The results of an analysis of (4.6) for $L = O(L_i)$ ($\varepsilon = O(1)$) are presented in table 1 in dimensional form. As is seen, the modes 1, 2, and 3 essentially differ. For $\Delta \ll 1$ (small perturbations of the bottom relief) σ_1 is close to the *barotropic* Rossby wave frequency, $-\beta k/\kappa^2$ in an ocean of constant depth. The large-scale velocity component is practically barotropic ($\bar{m} \simeq 1$), and the small-scale velocities generated by the bottom relief are small compared to the large-scale ones (Δ^{-1} times as small in the lower layer). Thus, for $\Delta \ll 1$ mode 1 practically coincides with the barotropic Rossby mode in a constant-depth ocean and is weakly affected by the stratification and bottom relief.

	$\Delta \ll 1$	$\Delta \sim 1$	$\Delta \gg 1$
σ_1	$-\frac{\beta k}{\kappa^2}$	$O\left(\frac{\beta k}{\kappa^2}\right)$	$-f_0 \frac{\Delta h}{h_2} \frac{k}{\kappa} \left(\frac{\alpha_1 + \kappa^2 L_i^2}{1 + \kappa^2 L_i^2}\right)^{1/2} \Sigma^{1/2}$
$\bar{m}_1$	1	$O(1), \quad \bar{m}_1 \neq 0, 1$	$1 + \alpha_1^{-1} \kappa^2 L_i^2$
r_1	$O(\Delta) \ll 1$	$O(1)$	$O(1)$
σ_2	$-\frac{\beta k}{\kappa^2 + L_i^{-2}}$	$O\left(\frac{\beta k}{\kappa^2}\right)$	$-\frac{\beta k}{\kappa^2 + f_0^2/g' h_1}$
$\bar{m}_2$	h_1/h_2	$O(1), \quad \bar{m}_2 \neq 0, 1$	$O(\Delta^{-2}) \ll 1$
r_2	$O(\Delta) \ll 1$	$O(1)$	$O(\Delta) \gg 1$
σ_3	$\frac{f_0^2}{\beta} \left(\frac{\Delta h}{h_2}\right)^2 \Sigma k$	$O\left(\frac{\beta k}{\kappa^2}\right)$	$+f_0 \frac{\Delta h}{h_2} \frac{k}{\kappa} \left(\frac{\alpha_1 + \kappa^2 L_i^2}{1 + \kappa^2 L_i^2}\right)^{1/2} \Sigma^{1/2}$
$\bar{m}_3$	$O(\Delta^{-2}) \gg 1$	$O(1), \quad \bar{m}_3 \neq 0, 1$	$1 + \alpha_1^{-1} \kappa^2 L_i^2$
r_3	$O(\Delta^{-1}) \gg 1$	$O(1)$	$O(1)$

TABLE 1. Characteristics of oscillation modes; $\Delta = (\Delta h/h_2)/(L/a)$.

Similarly, for $\Delta \ll 1$ mode 2 is close to the *baroclinic* Rossby mode in an ocean of constant depth, and the effect of the bottom relief on this mode is insignificant.

Mode 3 has the lowest frequency for $\Delta \ll 1$, and it degenerates in the absence of topography ($\sigma_3 \to 0$ as $\Delta h \to 0$). Thus, mode 3 exists owing to the perturbations of the bottom topography. The motion is confined to the lower layer, and the large-scale component is much weaker than the small-scale one.

When $\Delta = O(1)$, all three wave-producing factors (β-effect, topography and stratification) are of the same order, and modes 1, 2, 3 do not differ qualitatively. The frequencies σ_i, $i = 1, 2, 3$ are of the order of $\beta k/\kappa^2$, the large-scale components are baroclinic (in the sense that the large-scale velocities in the layers are different), and the large- and small-scale velocities are also of the same order.

The case of high bottom bumps, $\Delta \gg 1$, is most interesting. In this limit modes 1, 3 are weakly affected by the stratification and are transformed into high-frequency topographic oscillations with $\sigma_{1,3} = O\left(f_0(\Delta h/h_2)\right)$ (see above in this Section).

Mode 2 changes in a more unusual way. As is seen from table 1, the frequency σ_2 is close to the frequency of baroclinic Rossby waves in a two-layer ocean with infinitely deep immovable lower layer. The large-scale velocity in the upper layer greatly exceeds (Δ^2-fold) the lower layer large-scale velocity. We have $r = O(\Delta) \gg 1$, i.e. in the lower layer the amplitude of the small-scale velocity is larger than that of the large-scale velocity. At the same time, the product $\bar{m}r$ is of the order of $\Delta^{-1} \ll 1$, which means that the energy of the upper layer large-scale component is Δ^2 times as large as the total energy of the small-scale part of the velocity field. In other words, for $\Delta \gg 1$ the large-scale component in mode 2 dominates the small-scale one and is mainly confined to the upper layer.

The much weaker small-scale motion component is concentrated primarily in the lower layer and dominates the large-scale component here. As a result, the lower-layer fluid moves approximately along the isobaths, whereas motion in the upper layer can be directed arbitrarily. One can say that the large-scale component 'does not feel' the actual rough bottom and 'interprets' the interface as an 'effective' bottom. It is significant that the relative amplitude of small-scale motion *decreases* with increasing

amplitude $\Delta h/h_2$ of bottom bumps. Similar results can be obtained in the long wave limit $L \gg L_i$ (for a more detailed discussion see Reznik 1986). Note that $\sigma_2 = O(\beta L) = O(f_0\hat{\beta}/\hat{k})$ therefore $\Delta \gg 1$ means that the condition (2.10*b*) for strong topography is fulfilled for mode σ_2.

It readily follows from table 1 that the frequency of the surface-intensified mode σ_2 closed to $\sigma_2^{(s)}$ exceeds the flat-bottom baroclinic mode frequency $\sigma_2^{(f)}$ given wavevector $\boldsymbol{\kappa} = (k_x, k_y)$. Here we have

$$\sigma_2^{(s)} = \frac{-\beta k_x}{\kappa^2 + f_0^2/g'h_1}, \quad \sigma_2^{(f)} = \frac{-\beta k_x}{\kappa^2 + f_0^2/g'h_1 + f_0^2/g'h_2}.$$

The ratio $\sigma_2^{(s)}/\sigma_2^{(f)}$ is larger than unity and increases with decreasing κ; its maximum is equal to $(h_1 + h_2)/h_2$ (cf. Samelson 1992). One can say that mode σ_2 accelerates with increasing bottom bumps.

It is natural to call modes 1, 2, and 3 *barotropic, baroclinic, and topographic modes,* respectively.

The effects described are impossible in a homogeneous fluid, where, as readily follows from (4.2*a*), an increase in $\delta = \Delta h/h_2$ simply results in an increase of the oscillation frequency. This is also true for the barotropic and topographic modes 1 and 3, whose frequencies are weakly affected by stratification for small and large Δ. The frequencies $\sigma_{1,3}$ are $O\big(f_0(\Delta h/h_2)\big)$ for $\Delta \gg 1$, and therefore condition (2.10*a*) for moderate topography is satisfied for these modes. The motions in the upper and lower layers are of the same intensity, and the small- and large-scale lower-layer velocities are of the same order of magnitude.

Non-zonal isobaths: $\varphi \neq 0$

In terms of the variable $\tilde{\sigma}$ the dispersion relation (3.18) is reduced to (4.6) with the parameter Δ^2 replaced by $\tilde{\Delta}^2\Sigma$, where $\tilde{\Delta}^2 = \kappa\delta k/(\beta k_x)$ and Σ is given by (3.15). If

$$\beta/\sigma \ll 1, \tag{4.7}$$

then the terms proportional to β/σ can be neglected in (3.14*b*) and (3.15), and (3.18) practically coincides with (4.6) describing, as we saw, the barotropic, baroclinic, and topographic modes. One can readily show that (4.7) always holds for barotropic mode σ_1, the topographic mode σ_3 satisfies it for $\Delta \gtrsim 1$, and the baroclinic mode σ_2 satisfies it if $L = O(L_i)$.

Some other types of oscillations can take place on condition that

$$\beta/\sigma \gtrsim 1, \tag{4.8}$$

when the terms proportional to β/σ cannot be neglected in (3.14*b*) and (3.15). However, (4.8) together with (3.12) results in the relationship $k\delta \ll \sigma \lesssim \beta$, whence

$$\delta \ll L/a \ll 1. \tag{4.9}$$

Thus, the low-frequency oscillations satisfying (4.8) can be described by the asymptotic theory only for a very small relief inhomogeneity (by virtue of (4.9), $\delta \lesssim 0.01$). To analyse these modes for larger values of δ one has to use some other methods (see § 6).

Applicability of the asymptotic theory

The above consideration is valid only under condition (3.12), which can be verified for each of the modes. Let the amplitude of the depth perturbations be small,

$\delta \ll L/a$. It readily follows from table 1 that for the barotropic mode 1 we have $d \simeq (L_b/L)[\delta/(L/a)]$, and (3.12) is fulfilled. For the baroclinic mode 2 condition (3.12) can be rewritten as $\delta \ll L_i^2/(L_b a)$, i.e. the relations (3.12) and $\delta \ll L/a$ are satisfied for sufficiently small δ (this is also true in the long-wave limit $L \gg L_i$). For the topographic mode 3 the conditions (3.12) and $\delta \ll L/a$ hold simultaneously only if

$$\frac{L_b}{L} \ll \frac{\delta}{L/a} \ll 1,$$

i.e. for a sufficiently small bottom relief scale L_b ($L_b \lesssim 0.01L$).

In the case of a moderate depth perturbation $\delta = O(L/a)$ we have $d \simeq L_b/L \ll 1$ for all the modes, and (3.12) holds.

In the case of high bottom bumps when $\delta \gg L/a$ we have $d \simeq L_b/L \ll 1$ for the high-frequency barotropic and topographic modes, and (3.12) does not impose any additional constraints on the topography scale L_b. However, for the low-frequency baroclinic mode the relations (3.12) and $\delta \gg L/a$ hold simultaneously only if

$$1 \ll \frac{\delta}{L/a} \ll \frac{L_i}{L}\frac{L_i}{L_b}.$$

Hence, it follows (if, as usual, $\ll$ means at least 10-fold smaller) that $L_b \lesssim 0.01(L_i/L)L_i$, i.e. the asymptotic theory is valid only for very small L_b (for example, for $L = 100\,\mathrm{km}$ the scale L_b cannot exceed 1 km).

Thus, condition (3.12) is more restrictive for the baroclinic mode than for the barotropic and topographic ones. To investigate the baroclinic mode for larger values of L_b one must analyse the eigenvalue problem (2.7a, b) without condition (3.12). We managed to do this only for the periodic bottom topography. The next section is devoted to an asymptotic analysis of the baroclinic mode when $d = (k\delta)/\sigma = O(1)$ and (3.12) does not hold.

5. Asymptotic theory for the baroclinic mode over a strong periodic rough relief

To separate the baroclinic mode from the other modes in (2.7a, b) we set

$$\sigma = O(\beta L_i^2/L), \tag{5.1}$$

where σ and β are dimensional. Furthermore, we restrict ourselves to the case

$$L = O(L_i), \tag{5.2}$$

and therefore

$$q = O(k^2), \quad \frac{\beta k}{\sigma} = O(k^2). \tag{5.3}$$

Equations (2.7a, b) can be rewritten in the form

$$\psi_1'' - \mathrm{i}\bar{\beta}_2 k\psi_1' - n_1 k^2\psi_1 + \bar{\alpha}_1 k^2\psi_2 = 0, \tag{5.4a}$$

$$\psi_2'' - \mathrm{i}\bar{\beta}_2 k\psi_2' - (n_2 k^2 + d\bar{b})\psi_2 + \bar{\alpha}_2 k^2\psi_1 = 0, \tag{5.4b}$$

where

$$\left.\begin{gathered} \bar{\beta}_2 = \frac{\beta}{k\,\sigma}\sin\varphi = O(1), \quad n_i = \frac{k^2 + \alpha_i q + (\beta k/\sigma)cos\varphi}{k^2} = O(1), \\ \bar{\alpha}_i = \frac{\alpha_i q}{k^2} = O(1); \quad i = 1, 2, \quad \bar{b} = b'(y). \end{gathered}\right\} \tag{5.5}$$

We consider the case of a strong bottom relief and therefore put

$$d = \frac{k\delta}{\sigma} = O(1). \tag{5.6}$$

The system (5.4*a*, *b*) contains only one small parameter k, and the solution is sought in the following asymptotic form:

$$\psi_1 = \frac{1}{k}\bar{\psi}_1(Y) + \psi_1^{(0)}(y, Y) + k\psi_1^{(1)}(y, Y) + \dots , \tag{5.7a}$$

$$\psi_2 = \frac{1}{k}\bar{\psi}_2(Y) + \psi_2^{(0)}(y, Y) + k\psi_2^{(1)}(y, Y) + \dots . \tag{5.7b}$$

After some algebraic transformations the substitution of (5.7*a*, *b*) into (5.4*a*, *b*) results in

$$\psi_1^{(0)} = \psi_1^{(0)}(Y), \tag{5.8a}$$

$$\bar{\psi}_2 = 0, \tag{5.8b}$$

$$\bar{\psi}_{1YY} - \mathrm{i}\bar{\beta}_2\bar{\psi}_{1Y} - n_1\bar{\psi}_1 = 0, \tag{5.9a}$$

$$\psi_1^{(1)} = \psi_1^{(1)}(Y), \tag{5.9b}$$

$$\psi_{2yy}^{(0)} - d\bar{b}\psi_2^{(0)} = 0, \tag{5.9c}$$

$$\psi_{1YY}^{(0)} - \mathrm{i}\bar{\beta}_2\psi_{1Y}^{(0)} - n_1\psi_1^{(0)} + \psi_{1yy}^{(2)} + \bar{\alpha}_1\psi_2^{(0)} = 0, \tag{5.10a}$$

$$\psi_{2yy}^{(1)} - d\bar{b}\psi_2^{(1)} = -2\psi_{2yY}^{(0)} + \mathrm{i}\beta_2\psi_{2y}^{(0)} - \bar{\alpha}_2\bar{\psi}_1 = K_1, \tag{5.10b}$$

$$\psi_{1YY}^{(1)} - \mathrm{i}\bar{\beta}_2\psi_{1Y}^{(1)} - n_1\psi_1^{(1)} + \psi_{1yy}^{(3)} + 2\psi_{1yY}^{(2)} - \mathrm{i}\bar{\beta}_2\psi_{1y}^{(2)} + \bar{\alpha}_1\psi_2^{(1)} = 0, \tag{5.11a}$$

$$\psi_{2yy}^{(2)} - d\bar{b}\psi_2^{(2)} = -\left[\psi_{2YY}^{(0)} + 2\psi_{2yY}^{(1)} - \mathrm{i}\bar{\beta}_2(\psi_{2Y}^{(0)} + \psi_{2y}^{(1)}) - n_2\psi_2^{(0)} + \bar{\alpha}_2\psi_1^{(0)}\right] = K_2. \tag{5.11b}$$

Here the major difficulty is associated with (5.9*c*), (5.10*b*), and (5.11*b*), which cannot be solved easily for an arbitrary function $\bar{b} = \bar{b}(y)$. The analysis is somewhat simplified for a periodic bottom relief where $\bar{b}(y)$ is a periodic function. In this case one need not know *exact* analytical expressions for $\psi_2^{(0)}$, $\psi_2^{(1)}$, $\psi_2^{(2)}$ to determine the large-scale components $\bar{\psi}_1(Y)$, $\bar{\psi}_2(Y)$ and the dispersion relation. Instead, *general* properties of the ordinary differential equations with periodic coefficients (e.g. Smirnov 1974) can be used to do that.

The behaviour of the solutions to (5.9*c*) depends on the characteristic Lyapunov constant

$$A = \frac{\bar{R}_1(\omega) + \bar{R}_2'(\omega)}{2}, \tag{5.12}$$

where ω is the period of $\bar{b}$ and $\bar{R}_1$ and $\bar{R}_2$ are the linearly independent solutions to (5.9*c*) satisfying the initial conditions

$$\bar{R}_1(0) = 1, \quad \bar{R}_1'(0) = 0, \quad \bar{R}_2(0) = 0, \quad \bar{R}_2'(0) = 1. \tag{5.13}$$

Obviously given $\bar{b}(y)$ the parameter A is a function of the parameter d, i.e. $A = A(d)$. We now consider the following possible cases.

1. *The case* $|A| > 1$. For $|A| > 1$ the solutions to (5.9*c*) are unbounded for $y \to \pm\infty$, and two linearly independent solutions R_1, R_2 can be chosen in the form

$$R_1 = \mathrm{e}^{\lambda y}\varphi_1(y), \quad R_2 = \mathrm{e}^{-\lambda y}\varphi_2(y), \tag{5.14}$$

where λ is a real positive constant. In what follows φ_1, φ_2 are assumed to be some regular periodic functions with period ω. Note that R_1 and R_2 can differ from $\bar{R}_1$ and $\bar{R}_2$.

Since (5.9*c*) has no non-zero bounded solution, it follows that

$$\psi_2^{(0)} = 0. \tag{5.15a}$$

One can readily conclude from (5.8*a*), (5.10*a*), and (5.15*a*) that

$$\psi_{1YY}^{(0)} - \mathrm{i}\bar{\beta}_2\psi_{1Y}^{(0)} - n_1\psi_1^{(0)} = 0, \tag{5.15b}$$

$$\psi_1^{(2)} = \psi_1^{(2)}(Y). \tag{5.15c}$$

By virtue of (5.15*a*), the solution to (5.10*b*) takes the form

$$\psi_2^{(1)} = -\bar{\alpha}_2\bar{\psi}_1\int_0^\infty \mathrm{e}^{-\lambda s}\left[\varphi_1(y)\varphi_2(y+s) + \varphi_2(y)\varphi_1(y-s)\right]\mathrm{d}s; \tag{5.15d}$$

we will assume that the Wronskian of R_1 and R_2 is equal to 1, i.e.

$$W = R_1R_2' - R_1'R_2 = 1. \tag{5.16}$$

Equations (5.15*a*, *d*) indicate that the order of the large-scale velocity in the lower layer does not exceed $O(k^2)$, whereas in the upper layer it is of the order of 1. By virtue of (5.8*a*), (5.9*b*), and (5.15*c*), the small-scale velocity in the upper layer does not exceed $O(k^3)$, whereas in the lower layer it is $O(k)$. Thus, to within small values the motion is large scale and is confined to the upper layer. As before if the large-scale component is a plane wave, i.e. $\bar{\psi}_1$ is proportional to $\mathrm{e}^{\mathrm{i}lY}$, then one can obtain from (5.9*a*) the following (dimensional) dispersion relation:

$$\sigma = \frac{-\beta k_x}{k_x^2 + k_y^2 + f_0^2/g'h_1}. \tag{5.17}$$

Here k_x and k_y are the wave-vector components along the zonal and meridional directions, respectively. As could be expected, (5.17) coincides with the dispersion relation for Rossby waves in a two-layer ocean with an infinitely deep immovable lower layer.

So, we come to the conclusion that in the case $|A| > 1$ the mode is close to the baroclinic mode considered in §4 for $\Delta \gg 1$.

2. *The cases* $|A| < 1$ *and* $A = -1$. If $|A| < 1$, then all solutions to (5.9*c*) are bounded for $-\infty \leqslant y \leqslant \infty$, and the pair of linearly independent solutions takes the form

$$R_1 = \mathrm{e}^{2\mathrm{i}\pi\alpha y/\omega}\varphi_1(y), \quad R_2 = \mathrm{e}^{-2\mathrm{i}\pi\alpha y/\omega}\varphi_2(y), \tag{5.18}$$

where α is real, $\alpha \neq 0, 1$. For $A = -1$ we have $\alpha = 1/2$ and $\varphi_2(y) = \varphi_1^*(y)$ in (5.18). Respectively, the solution to (5.9*c*) can be written as

$$\psi_2^{(0)} = C_1^{(0)}(Y)R_1 + C_2^{(0)}(Y)R_2, \tag{5.19}$$

where and $C_1^{(0)}$ and $C_2^{(0)}$ are arbitrary functions.

To obtain $\psi_1^{(0)}$, $\psi_2^{(0)}$ we use the equations

$$\langle R_1 \rangle = \langle R_2 \rangle = 0 \tag{5.20}$$

which simply follows from the formula (A 3) of Appendix A. On averaging (5.10*a*) with respect to y and applying (5.20) we derive

$$\psi_{1YY}^{(0)} - \mathrm{i}\bar{\beta}_2 \psi_{1Y}^{(0)} - n_1 \psi_1^{(0)} = 0, \tag{5.21a}$$

$$\psi_{1yy}^{(2)} = -\bar{\alpha}_1 \psi_2^{(0)}. \tag{5.21b}$$

The functions $C_1^{(0)}(Y)$ and $C_2^{(0)}(Y)$ are determined from the condition of boundedness of $\psi_2^{(1)}$ for $-\infty \leqslant y \leqslant \infty$. This condition is satisfied if and only if the right-hand side of (5.10*b*) is orthogonal to R_1 and R_2, i.e.

$$\langle K_1 R_1 \rangle = \langle K_1 R_2 \rangle = 0. \tag{5.22}$$

Taking into account (A 3), (5.19), and (5.16) we conclude from (5.22) that

$$C_k^{(0)} = M_k^{(0)} \mathrm{e}^{(\mathrm{i}\bar{\beta}/2)Y}, \quad k = 1, 2, \tag{5.23}$$

where $M_k^{(0)}$, $k = 1, 2$, are some constants.

In view of (5.23), the solution $\psi_2^{(1)}$ to (5.10*b*) can be written as

$$\psi_2^{(1)} = -\bar{\alpha}_2 \bar{\psi}_1 F_0(y) + C_1^{(1)}(Y) R_1 + C_2^{(1)}(Y) R_2 \tag{5.24}$$

where $C_1^{(1)}$, $C_2^{(1)}$ are arbitrary functions. The function F_0 is a particular solution of the equation

$$F'' - d\bar{b} F = 1 \tag{5.25}$$

and has the form

$$F = -R_1 \int R_2(y')\,\mathrm{d}y' + R_2 \int R_1(y')\,\mathrm{d}y'. \tag{5.26}$$

One can show (see Appendix A for details) that the functions $C_1^{(1)}(Y)$ and $C_2^{(1)}(Y)$ are bounded in Y if and only if $M_1^{(0)}$ and $M_2^{(0)}$ are equal to zero, i.e.

$$\psi_2^{(0)} = 0, \tag{5.27}$$

and, by virtue of (5.21*b*),

$$\psi_1^{(2)} = \psi_1^{(2)}(Y). \tag{5.28}$$

Thus in the cases under consideration the structure of the mode is identical to that for $|A| > 1$.

3. *The case* $A = 1$. If $A = 1$ the solutions R_1 and R_2 can be represented as

$$R_1 = \varphi_1(y), \quad R_2 = ay\varphi_1(y) + \varphi_2(y), \tag{5.29}$$

i.e. one solution is bounded and the other is unbounded. A detailed analysis of this case is given in Appendix A, here only the qualitative results are presented.

The structure of the motion depends strongly on the parameter $\langle R_1 \rangle$. If $\langle R_1 \rangle = 0$ then the large-scale motion in the upper layer described by (5.9*a*) and the dispersion relation (5.17) remain unchanged. At the same time, motion in the lower layer is intensified in comparison with the foregoing cases: here the small-scale velocity is of the order of the large-scale velocity in the upper layer.

If $\langle R_1 \rangle \neq 0$ the motion has a completely different structure in comparison with the

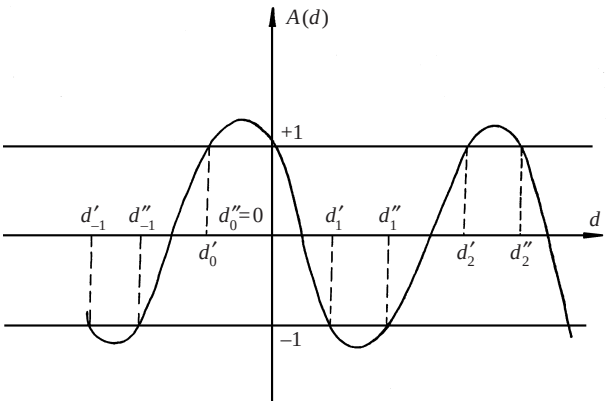

FIGURE 2. Schematic representation of the dependence of the Lyapunov constant A on the parameter d in the Hill equation (5.9c).

above cases. The function $\bar{\varphi}_1(Y)$ in (5.7a) vanishes and, therefore, the upper layer velocity amplitude is of the order of k. In the lower layer the large-scale component is also of the order of k and the small scale component is of the order of 1. Thus, the motion is mainly small scale and confined to the lower layer. The corresponding dispersion relation differs strongly from (5.17).

The above analysis can be briefly summarized as follows. For $A \neq 1$ the motion in the mode is predominantly large scale and confined mainly to the upper layer; the lower layer velocity is small scale and much smaller in magnitude than the upper layer velocity. Correspondingly, the dispersion relation in this case is given by (5.17) coinciding with the dispersion relation for Rossby waves in a two-layer ocean with an infinitely deep immovable lower layer.

In contrast to this, if $A = 1$ then the small-scale motion in the lower layer is intensified so that the lower layer small-scale velocity is of the order or larger than the large-scale components in the layers. The dispersion relation can strongly differ from (5.17) in this case.

We now consider the properties of the function $A(d)$ given the function $\bar{b}(y)$ in (5.9c) (Smirnov 1974).

(i) Each of the equations $A(d) = 1$ and $A(d) = -1$ has a countable set of real roots.

(ii) These roots can be indexed so that

$$\ldots, d'_{-1} \leqslant d''_{-1} < d'_0 \leqslant d''_0 = 0 < d'_1 \leqslant d''_1 < d'_2 \leqslant d''_2 < d'_3 \leqslant d''_3 \ldots,$$

where $\ldots, d'_0, d''_0 = 0, d'_2, d''_2, d'_4, d''_4, \ldots$ are the roots of the equation $A(d) = 1$ and $\ldots, d'_{-1}, d''_{-1}, d'_1, d''_1, d'_3, d''_3, \ldots$ are the roots of the equation $A(d) = -1$. Here $\ldots, (d''_0, d'_1), (d''_1, d'_2), (d''_2, d'_3), \ldots$ are the intervals of boundedness ($|A(d)| < 1$ in these intervals) and $\ldots, (d'_{-1}, d''_{-1}), (d'_0, d''_0), (d'_1, d''_1), \ldots$ are the intervals of unboundedness ($|A(d)| > 1$ in them).

(iii) The function $A(d)$ is monotonic in the intervals of boundedness ($A'(d) > 0$ or $A'(d) < 0$).

Dependence A versus d is presented in figure 2.

It is convenient to state the results in terms of the phase velocity

$$c_x = \frac{\sigma}{k} \tag{5.30}$$

along the isobaths. The dependence of A on d leads to the conclusion that cases 1 and 2 are realized for almost all c_x, and therefore the motion under consideration is mainly large scale and is confined to the upper layer of the ocean. The exceptions are the following values of phase velocity c_x:

$$c_x = \frac{\delta}{d'_n} \quad \text{or} \quad c_x = \frac{\delta}{d''_n}, \quad n = \pm 2m. \tag{5.31}$$

A kind of resonance appears for such c_x when a relatively weak large-scale wave generates a small-scale velocity field with an amplitude much greater than that of the large-scale component. However, this effect seems to be unimportant dynamically because only a countable set of c_x satisfies (5.31), whereas a continuum of c_x does not satisfy (5.31). Moreover, the distance between the consecutive values of d satisfying (5.31) is of the order of 1, and d is of the order of 1 here (see (5.6)).

Thus, the characteristics of the baroclinic mode over a strong bottom relief described in § 4 for $d \ll 1$ are realized also in the case $d = O(1)$. In other words, the main result of this Section is that for the case of a strong periodic bottom relief when (5.6) is fulfilled the baroclinic mode is closed to the Rossby wave in a two-layer ocean with an infinitely deep lower layer. This result does not depend on the exact form of the topography, only its periodicity is of importance.

We now evaluate the characteristic scales of motion and bottom topography for which the above analysis is valid. Let the scale L be of the order of 100 km, then for $k = 0.1$ the horizontal bottom topography scale $L_b = 10$ km. By virtue of (5.17), we have $\sigma = O(0.01)$, and therefore the condition $d = O(1)$ implies $\delta = O(0.1)$. For the typical depth of the lower layer equal to 4 km the characteristic height of the bottom inhomogeneities is equal to 400 m. Clearly, these scales correlate well with those of the actual bottom relief and mesoscale motion in the ocean.

The above asymptotic consideration relates only to the case of a rough-bottomed topography. If the bottom relief is not rough and the non-dimensional wavenumber $\hat{k}$ in (2.7a, b) is not necessarily small, then the eigenvalue problem (2.7a, b) becomes much more complicated because asymptotic methods cannot be applied in this case. However, the periodic bottom relief can be analysed using the results of the general theory of ordinary differential equations with periodic coefficients. The investigation technique and the results for a sinusoidal bottom topography are presented in the next Section.

6. Waves over a sinusoidal bottom relief

To analyse the eigenvalue problem (2.7a, b) for the case of a periodic bottom relief with period ω we rewrite the system in the form of the vector equation

$$\frac{\mathrm{d}\boldsymbol{x}}{\mathrm{d}y} = \boldsymbol{A}(y)\boldsymbol{x}, \tag{6.1}$$

for the four-dimensional vector

$$\boldsymbol{x} = \begin{pmatrix} \psi_1 \\ \psi_2 \\ \psi_3 \\ \psi_4 \end{pmatrix}, \quad \psi_3 = \psi'_1, \quad \psi_4 = \psi'_2, \tag{6.2}$$

where $\boldsymbol{A}(y)$ is a periodic 4×4 matrix with period ω. Using the investigation technique presented in Appendix B we can find the k, σ, δ, and q for which the system (6.1) has bounded solution, and calculate these solutions.

Each of these solutions can be represented as

$$\boldsymbol{x}(y) = \mathrm{e}^{\mathrm{i}ly}\boldsymbol{f}(y), \tag{6.3}$$

where $\boldsymbol{f}(y)$ is a periodic four-dimensional vector and l is a constant. Knowing l and $\boldsymbol{f}(y)$ we can determine the large- and small-scale components of motion proportional to

$$\bar{\boldsymbol{x}}(y) = \mathrm{e}^{\mathrm{i}ly}\bar{\boldsymbol{f}} = \begin{pmatrix} \bar{\psi}_1 \\ \vdots \\ \bar{\psi}_4 \end{pmatrix} \tag{6.4a}$$

and

$$\tilde{\boldsymbol{x}}(y) = \mathrm{e}^{\mathrm{i}ly}\tilde{\boldsymbol{f}} = \begin{pmatrix} \tilde{\psi}_1 \\ \vdots \\ \tilde{\psi}_4 \end{pmatrix}, \tag{6.4b}$$

respectively. Here we have

$$\bar{\boldsymbol{f}} = \frac{1}{\omega}\int_0^{\omega} \boldsymbol{f}(y)\,\mathrm{d}y; \quad \tilde{\boldsymbol{f}} = \boldsymbol{f}(y) - \bar{\boldsymbol{f}}, \tag{6.5}$$

$$\boldsymbol{x} = \bar{\boldsymbol{x}} + \tilde{\boldsymbol{x}}. \tag{6.6}$$

Using (6.4a, b) one can calculate the coefficients (3.19) characterizing the vertical structure of the motion and the relationship between the large- and small-scale components. Of course, this representation makes sense only when $l \ll 1$; otherwise the large- and small-scale components are of the same spatial scale.

Oscillations in a barotropic ocean can be investigated in a similar manner if we equate α_1 and α_2 in (2.7a, b) to zero. In this case equations (2.7a) and (2.7b) decouple and (2.7b) is transformed into an equation describing waves in a barotropic ocean of variable depth in the rigid-lid approximation (e.g. see Kamenkovich & Reznik 1978). To study these waves one should find bounded solutions ψ_1 and ψ_2 to system (2.7a, b) with $\alpha_1 = \alpha_2 = 0$ and discard the 'parasitic' mode ψ_1.

The analysis was carried out for a cosinusoidal bottom relief, i.e. $\hat{b}' = \sin y$ in (2.7b). The following parameters were chosen: $f_0 = 7 \times 10^{-5}\,\mathrm{s}^{-1}$, $\beta = 1.8 \times 10^{-13}\,\mathrm{sm}^{-1}\,\mathrm{s}^{-1}$, $\alpha_1 = 0.75$, $\alpha_2 = 0.25$, and $L_i = 43\,\mathrm{km}$. The results can be stated conveniently in terms of the wavelength $\lambda_x = 2\pi/k$ and the period $T = 2\pi/\sigma$. The calculations were performed for a rectangular grid covering the domain $-1500\,\mathrm{km} \leqslant \lambda_x \leqslant 1500\,\mathrm{km}$, $20\ \mathrm{days} \leqslant T \leqslant 400\ \mathrm{days}$ with steps $\Delta\lambda_x = 100\,\mathrm{km}$ and $\Delta T = 20$ days; obviously, the characteristic scales of the observed mesoscale eddies lie in these ranges. The results are demonstrated in figures 3–6; each symbol (cross or dot) designates the 'allowable' values of T and λ_x for which bounded solutions to (2.7a, b) exist.

One can readily see that not all values of T and λ_x are allowable. In the barotropic case (figure 3) there exist two domains I and II corresponding to the topographic and barotropic modes, respectively. In the two-layer case region III of baroclinic oscillations is added to regions I and II (figures 4, 5). For a given δ with increasing bottom topography scale L_b all allowable domains of oscillations decrease, and domains I and II of topographic and barotropic modes degenerate much more quickly than domain III of baroclinic modes. At the same time, all the allowable

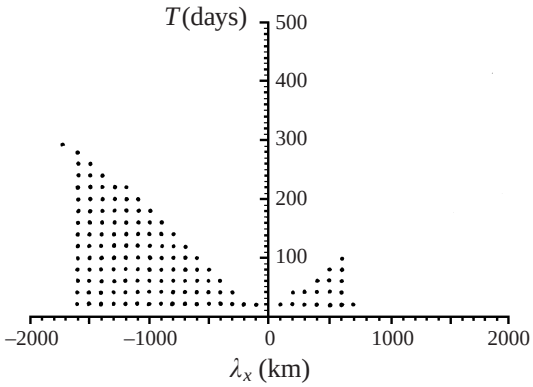

FIGURE 3. The domains of allowable periods T and wavelengths λ_x for the barotropic ocean; $\delta = 0.1$, $L_b = 4\,\mathrm{km}$, $\varphi = 0$.

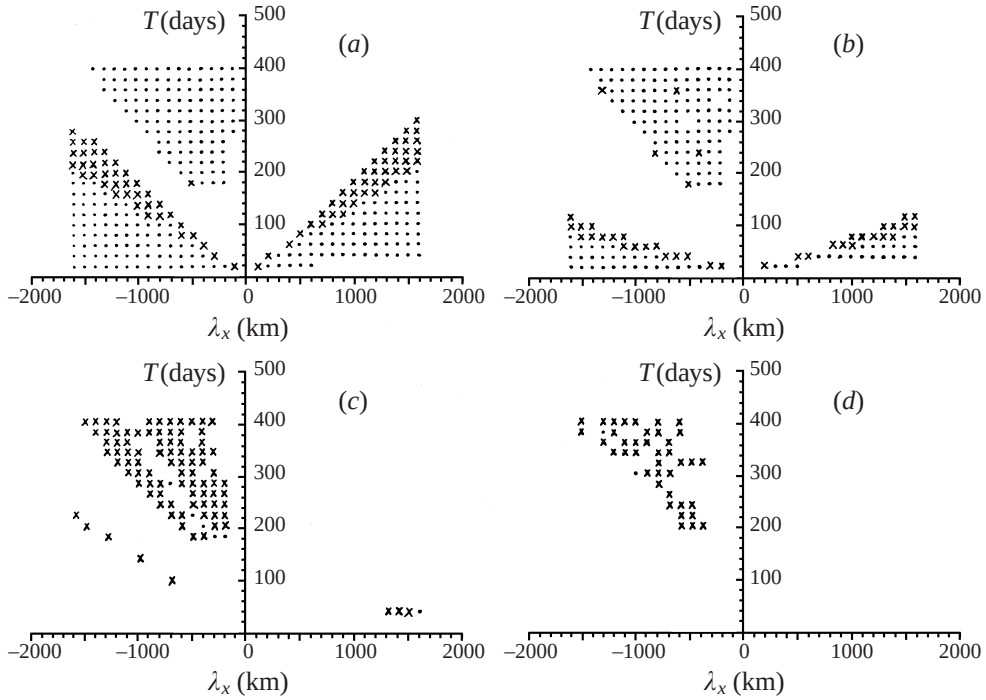

FIGURE 4. The same as figure 3 except for the two-layer ocean; $\delta = 0.1$. Different symbols characterize level of the relative error M of the asymptotic wavenumber (6.12): dots correspond to $M \leqslant 20\%$. (*a*) $L_b = 4\,\mathrm{km}$; (*b*) $L_b = 10\,\mathrm{km}$; (*c*) $L_b = 40\,\mathrm{km}$; (*d*) $L_b = 100\,\mathrm{km}$.

domains increase with decreasing relative height of the bottom inhomogeneities (see figures 4, 5 and 6). Note that the subdivision of the (T, λ_x) plane into regions of barotropic, topographic, and baroclinic modes is clearly seen only in the case of zonal isobaths; if the isobaths are not parallel to the zonal direction, then the barotropic and topographic domains are not separated well (figure 6). It is also interesting that, generally, the number of the allowable T, λ_x is larger in the case of non-zonal isobaths (compare figures 4, 5 and 6).

To check the applicability of the asymptotic dispersion relation (3.18) we rewrite it

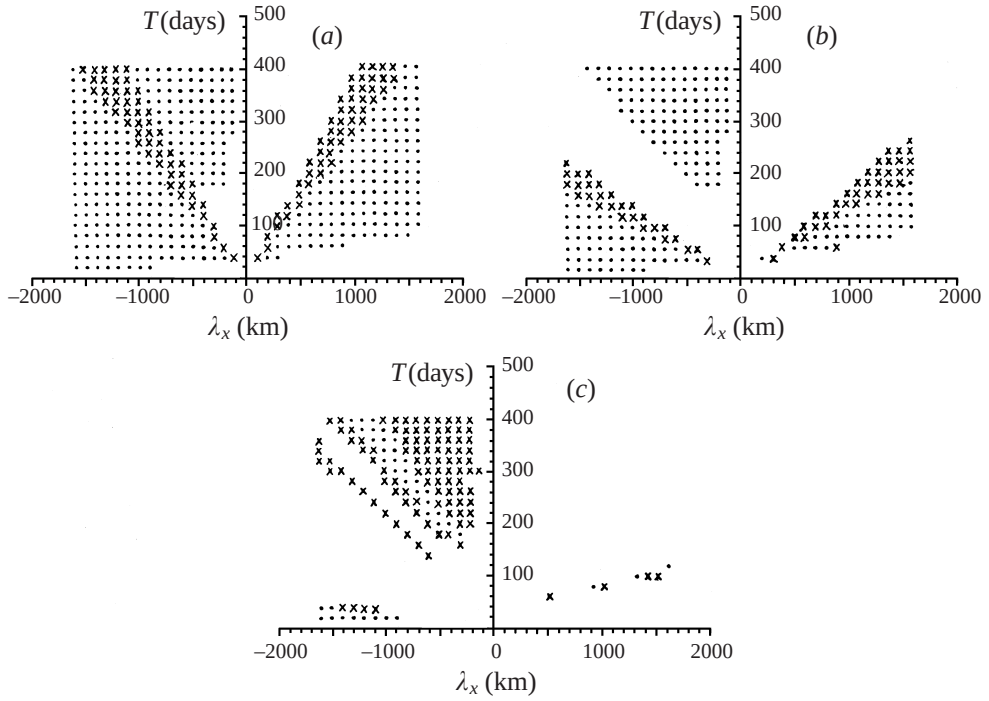

FIGURE 5. The same as figure 4 except for $\delta = 0.05$. (*a*) $L_b = 4\,\mathrm{km}$; (*b*) $L_b = 10\,\mathrm{km}$; (*c*) $L_b = 40\,\mathrm{km}$.

in the form of the dependence of the wavenumber l on the parameters k and σ:

$$l_a = \frac{\beta}{2\sigma}\sin\varphi \pm \left(\frac{\beta^2}{4\sigma^2}\sin^2\varphi - k^2 - \frac{\beta k}{\sigma}\cos\varphi + B(k,\sigma)\right)^{1/2}, \tag{6.7a}$$

where

$$B = B(k,\sigma) = \frac{1}{2}\left(\frac{\delta^2k^2}{\sigma^2}\Sigma - q\right) \pm \left(\frac{1}{4}\left(\frac{\delta^2k^2}{\sigma^2}\Sigma - q\right)^2 + \alpha_1 q\frac{\delta^2k^2}{\sigma^2}\Sigma\right)^{1/2}. \tag{6.7b}$$

The subscript a means that the wavenumber l_a is calculated by the asymptotic theory. Given $\bar{k}$ and σ, we calculate the 'asymptotic' wavenumber l_a from (6.7) and the exact value $l_T = l$ from (6.3), and then the parameter M,

$$M = \frac{|l_T - l_a|}{l_T},$$

which can be interpreted as the error of the asymptotic expression (6.7). One can see from figures 4, 5, and 6 that for moderate L_b (4 km, 10 km) the dispersion relation (6.7) holds to within small errors in the major part of the (T, λ_x)-domain, especially for the baroclinic modes, even for sufficiently large $d = k\delta/\sigma$ when the condition (3.12) is violated. With increasing L_b the error M increases and becomes large for $L_b = 40\,\mathrm{km}$, 100 km (although for these values of L_b there also exist T and λ_x for which (6.7) is satisfied with a good accuracy).

We also calculated the coefficients (3.19) for the exact and asymptotic solutions and compared them. Using (3.13) for the cosinusoidal relief we obtain for the asymptotic

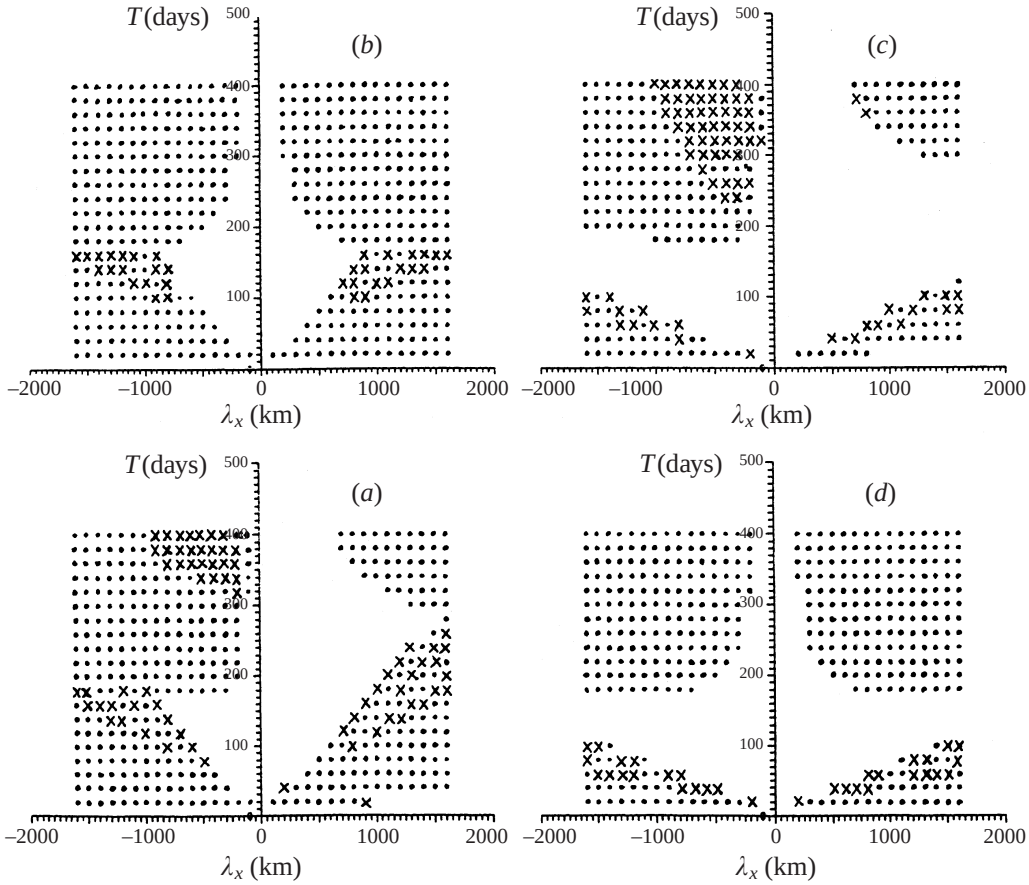

FIGURE 6. The same as figure 4 except for $\varphi \neq 0$. (*a*) $L_b = 4\,\text{km}$, $\varphi = 45°$; (*b*) $L_b = 4\,\text{km}$, $\varphi = 90°$; (*c*) $L_b = 10\,\text{km}$, $\varphi = 45°$; (*d*) $L_b = 10\,\text{km}$, $\varphi = 90°$.

solution:

$$\tilde{m} = 1 + \frac{1}{\alpha_1 q}, \quad r = \frac{k\delta}{\kappa\sigma}\frac{1}{\sqrt{2}}\frac{1+\alpha_1 q}{1+q}; \tag{6.8}$$

the parameter $\bar{m}$ is given by (3.20*a*). The coefficients (3.19) for different values of L_b and δ are shown in table 2 for the topographic, barotropic and baroclinic modes. One can see from table 2 and figures 4 and 5 that the vertical structure of the modes is adequately described by the approximate coefficients (3.20*a*) and (6.8) even in the case when $k\delta/\sigma \gtrsim 1$ and the condition (3.12) does not hold. We emphasize that the most interesting and important effects, namely the 'screening' effect (the concentration of the small-scale component generated by the relief with scale $L_b < L_i$ in the lower layer) and the 'displacement' effect (the baroclinic mode over a strong relief is confined mainly to the upper layer), also occur for $k\delta/\sigma \gtrsim 1$ even when the wave scale L slightly exceeds the relief scale L_b (for example, see the case $L_b = 40\,\text{km}$, $\delta = 0.1$, $\lambda_x = -400\,\text{km}$, $T = 180$ days). The 'displacement' effect can exist even if the scale L is equal to L_b. For example, as can be seen from table 2, in the case $L_b = 100\,\text{km}$, $\delta = 0.1$, $\lambda_x = -400\,\text{km}$, $T = 200$ days the motion with scale L_b dominates in the mode and the relative intensity of motion in the layers is determined primarily by the

parameter $\tilde{m}_T$. This parameter is equal to 0.3, i.e. the kinetic energy level in the upper layer is approximately ten times as large as that in the lower one.

7. Discussion and conclusions

Motivation of this work was to gain an understanding of the joint effect of stratification, β-effect, and bottom topography on the quasi-geostrophic oceanic motion. Most of previous works restricted their consideration to the case of moderate topography when

$$\frac{\Delta h}{H} \lesssim \max(\varepsilon_T, Ro, \varepsilon_R). \tag{7.1}$$

However this condition certainly does not hold in the regions with abrupt topography where the condition

$$\frac{\Delta h}{H} \gg \max(\varepsilon_T, Ro, \varepsilon_R) \tag{7.2}$$

of strong topography is satisfied for the low-frequency mesoscale motion.

To study the problem in the simplest form we have investigated linear Rossby waves in a two-layer ocean with a corrugated bottom relief (the isobaths are parallel straight lines). The asymptotic theory developed for the rough relief is valid over a wide range of the parameters L_b/L, L/a, L_b/L_i, and $\Delta h/h_2$, and allows both the moderate and strong topography cases to be described. As could be expected, the combined effect of the stratification and bottom topography results in an increase in the number of possible wave modes compared to the cases of two-layer ocean of constant depth or a barotropic ocean of variable depth. There exist three types of modes: barotropic, topographic and baroclinic. As $\Delta h \to 0$ the barotropic and baroclinic modes are transformed into the 'usual' barotropic and baroclinic Rossby modes, respectively. At the same time the topographic mode degenerates in the limit of constant depth because its frequency tends to zero for $\Delta h \to 0$.

The structure and frequencies of the modes depend substantially on the ratio $\Delta = (\Delta h/h_2)/(L/a)$ measuring the relative strength of the topography and the β-effect. The topographic and barotropic modes are weakly affected by the stratification, and their frequencies increase monotonically with increasing Δ. For $\Delta \gg 1$ these frequencies are $O\big(f_0(\Delta h/h_2)\big)$, and therefore the condition (1.11a) of moderate topography is satisfied for the barotropic and topographic modes even for a large height of the relief inhomogenity. Both the modes become close to pure topographic modes for large $\Delta h/h_2$ when $\Delta \gg 1$.

The dependence of the baroclinic mode on Δ is more non-trivial. The frequency of this mode is of the order of $\beta k L_i^2$ irrespective of the height of the relief inhomogeneity. At the same time, the spatial structure of the mode strongly depends on $\Delta h/h_2$. With increasing Δ the relative magnitude of the motion in the lower layer decreases. If the relief inhomogeneity is large so that $\Delta \gg 1$, then the motion in the lower layer is very weak and the baroclinic mode is close to a Rossby wave in a two-layer ocean with an infinitely deep immovable lower layer.

The case $\Delta \gg 1$ or, alternatively, $\Delta h/h_2 \gg L/a$ coincides for this mode with the condition (1.11b) of the strong bottom relief because $\beta k L_i^2 \leqslant f_0(L/a)$ and therefore $\varepsilon_T \leqslant \varepsilon_R$ in (1.11b). Thus, the baroclinic mode is predominantly large scale and is confined to the upper layer over the strong bottom relief. The much weaker small-scale component of motion is concentrated mainly in the lower layer and dominates there over the large scale component. As a result, the lower layer fluid moves approximately

Relief parameters	Mode	x-wave-length (km)	Period (day)	$\bar{m}_t$	$\bar{m}_a$	$\tilde{m}_t$	$\tilde{m}_a$	r_t	r_a	$d = k\delta/\sigma$
$L_b = 4$ km,	barotropic	−400	20	1.97	1.97	150.9	155.1	0.9879	0.9993	0.121
$\delta = 0.1$	baroclinic	−400	180	0.0033	0.0035	122.6	155.1	12.57	11.27	1.09
	topographic	400	20	1.96	1.96	154.7	155.1	1.21	1.23	0.121
$L_b = 10$ km,	barotropic	−400	20	2.01	2.01	21.93	25.65	0.99	1.06	0.3
$\delta = 0.1$	baroclinic	−400	180	0.0015	0.0016	27.59	25.65	36.4	12.16	2.72
	topographic	400	20	1.94	1.94	25.45	25.65	1.21	1.35	0.3
$L_b = 40$ km,	baroclinic	−400	180	0.063	0.063	5.42	0.54	8.38	35.6	10.9
$\delta = 0.1$	baroclinic	−400	200	0.00047	0.0008	0.57	25.4	396.9	337.3	12.1
$L_b = 100$ km, $\delta = 0.1$	baroclinic	−400	200	0.33	0.32	0.3	1.25	18.52	438.1	30.24
$L_b = 4$ km,	barotropic	−400	40	1.976	1.975	149.0	155.1	0.916	0.923	0.121
$\delta = 0.05$	barotropic	−400	140	24.06	24.04	62.79	155.1	1.03	0.764	0.42
	baroclinic	−400	180	0.014	0.014	143.2	155.1	5.8	5.67	0.54
	topographic	400	60	3.33	3.33	147	155.1	1.21	1.21	0.18
$L_b = 10$ km,	barotropic	−400	40	2.05	2.05	20.39	25.65	0.93	0.97	0.3
$\delta = 0.05$	baroclinic	−400	180	0.012	0.012	24.56	25.65	7.2	6.1	1.35
	topographic	400	60	3.59	3.59	19.11	25.65	1.18	1.23	0.45
$L_b = 40$ km, $\delta = 0.05$	baroclinic	−400	180	0.019	0.019	3.65	2.54	13.13	16.8	5.44

TABLE 2. The parameters characterizing the vertical and horizontal structure of the modes. Subscripts a and t denote the parameters calculated by the asymptotic theory and numerically, respectively.

along the isobaths, whereas the motion in the upper layer can be directed arbitrarily. One can say that the baroclinic mode over a strong bottom relief does not 'feel' the actual uneven bottom and 'interprets' the interface between the layers as a bottom.

It is of importance that the surface intensification of the baroclinic mode with increase of the relief height is accompanied by some increase of the mode frequency (see Samelson 1992, 1998). An analogous effect takes place in a continuously stratified ocean (Bobrovich & Reznik 1999). Note that the observed 'fast' Rossby waves propagation (Chelton & Shlax 1996) could be due to the topographic alteration of the lowest baroclinic mode.

The asymptotic theory was developed under the assumption that the horizontal scale L_b of the relief inhomogeneity does not exceed the Rossby internal scale L_i. To verify and generalize these results we developed a method making it possible to investigate oscillations over an arbitrary periodic bottom relief. The calculation demonstrates a decrease in the number of possible oscillations with increasing $\Delta h/h_2$ and especially with increasing horizontal bottom scale L_b. For example, the barotropic and topographic modes are almost absent for $L_b \geqslant L_i$; the low-frequency baroclinic modes are more 'persistent': they exist for any L_b. The effect of concentration of motion in the upper layer with increasing $\Delta h/h_2$ (the 'displacement' effect) also occurs for $L_b \geqslant L_i$ although this concentration can be less strong than in the case of a rough relief with $L_b \ll L_i$. It is significant that a similar concentration of the mesoscale motion in the upper layer over an abrupt bottom topography has been observed many times in the real ocean (e.g. see Wunsch 1981, 1983; Dickson 1983).

Another important physical effect is the so-called 'screening' effect. It implies that for $L_b < L_i$ the small-scale component of the wave is confined to the lower layer, whereas in the upper layer the scale of motion L is always greater than or of the order of L_i (also see McWilliams 1974; Zhdanov 1987). In other words, the stratification prevents the ingress of motion with scale smaller than the internal Rossby scale into the main thermocline.

Obviously the above theory becomes inapplicable for the cases of a random and/or two-dimensional bottom topography. The analyses by Sengupta *et al.* (1992); Rhines & Bretherton (1973) show that such topographies cannot support the propagation of large-scale quasi-geostrophic oscillations in the barotropic ocean; instead a localization in the horizontal of the waves occurs. As we have seen the stratification depresses the effect of topography on the upper layer; therefore in stratified fluid the localization of the upper layer motion could be substantially weaker than in the barotropic case. Some numerical simulations for a stratified ocean with a broad spectrum topography are required to gain more understanding of this problem.

We have considered only the simplest two-layer stratification. Generalization to the continuously stratified case is reported in a companion paper (Bobrovich & Reznik 1999).

This work was supported by grants from the Russian Foundation of Basic Research (94-05-17538a, 96-05-65209). The authors wish to thank Professor V. M. Volosov for very helpful comments on the manuscript and M. V. Dmitrieva and L. I. Voronovich for the help in preparation of this manuscript.

Appendix A

Let us consider the function

$$Q = \mathrm{e}^{2\mathrm{i}\pi\alpha y/\omega} p(y), \tag{A 1}$$

where $p(y)$ is a regular periodic function with period ω; α is real,

$$\alpha \neq 0, 1. \tag{A 2}$$

The condition (A 2) means that the Fourier series for $p(y)$ does not contain the harmonic $\mathrm{e}^{2\mathrm{i}\pi\alpha y/\omega}$ i.e.

$$\langle Q \rangle = \langle \mathrm{e}^{2\mathrm{i}\pi\alpha y/\omega} p(y) \rangle = 0. \tag{A 3}$$

To derive (5.27) we use the Fourier series for R_1 and R_2 to calculate the antiderivatives in (5.26):

$$R_1 = \sum_m A_1^{(m)} \mathrm{e}^{2\pi\mathrm{i}(m+\alpha)y/\omega}, \quad R_2 = \sum_n A_2^{(n)} \mathrm{e}^{2\pi\mathrm{i}(n-\alpha)y/\omega}. \tag{A 4}$$

Substituting (A 4) into (5.26) we obtain after some simple algebra a particular solution to (5.25):

$$F_0 = \frac{\omega}{2\pi\mathrm{i}} \sum_{m,n} \frac{A_1^{(m)} A_2^{(n)} (n-m-2\alpha)}{(m+\alpha)(n-\alpha)} \mathrm{e}^{2\pi\mathrm{i}(m+n)y/\omega}, \tag{A 5}$$

which is a periodic function with period ω.

The functions $C_1^{(1)}(Y)$ and $C_2^{(1)}(Y)$ in (5.24) are determined from the orthogonality of the right-hand side of (5.11*b*) to R_1 and R_2:

$$\langle K_2 R_1 \rangle = \langle K_2 R_2 \rangle = 0. \tag{A 6}$$

Taking into account (5.8*a*), (5.16), (5.19), (5.23), (A 3), and (A 5) we derive from (A 6) equations for $C_1^{(1)}(Y)$ and $C_2^{(1)}(Y)$:

$$C_{1Y}^{(1)} - \mathrm{i}\frac{\bar{\beta}_2}{2} C_1^{(1)} = \left(\frac{\bar{\beta}_2^2}{4} - n_2\right) \left(M_1^{(0)} \langle R_1 R_2 \rangle + M_2^{(0)} \langle R_2^2 \rangle\right) \mathrm{e}^{\mathrm{i}(\bar{\beta}_2/2)Y}, \tag{A 7}$$

$$C_{2Y}^{(1)} - \mathrm{i}\frac{\bar{\beta}_2}{2} C_2^{(1)} = -\left(\frac{\bar{\beta}_2^2}{4} - n_2\right) \left(M_1^{(0)} \langle R_1^2 \rangle + M_2^{(0)} \langle R_1 R_2 \rangle\right) \mathrm{e}^{\mathrm{i}(\bar{\beta}_2/2)Y}. \tag{A 8}$$

For non-zero $M_1^{(0)}$ and $M_2^{(0)}$ the functions $C_1^{(1)}(Y)$ and $C_2^{(1)}(Y)$ are bounded in Y if and only if

$$\left(\frac{\bar{\beta}_2^2}{4} - n_2\right)^2 \left(\langle R_1^2 \rangle \langle R_2^2 \rangle - \langle R_1 R_2 \rangle^2\right) = 0. \tag{A 9}$$

It follows from the boundedness of $\psi_1^{(0)}$ for $-\infty < Y < +\infty$ that $\bar{\beta}_2^2/4 - n_2 > 0$ (see (5.21*a*)). Furthermore, assuming that $R_2 = R_1^*$ and using the Cauchy–Holder inequality one can show that $\langle R_1^2 \rangle \langle R_2^2 \rangle - \langle R_1 R_2 \rangle^2 < 0$. Thus, (A 9) does not hold, and therefore $M_1^{(0)}$ and $M_2^{(0)}$ are equal to zero, whence (5.27) follows.

In the case $A = 1$ the bounded solution to (5.9*c*) has the form

$$\psi_2^{(0)} = C_1^{(0)}(Y) R_1. \tag{A 10}$$

Let us assume that in (5.29)

$$\langle R_1 \rangle = 0. \tag{A 11}$$

Using (A 10), (A 11) one can readily obtain from (5.10*a*) the equations (5.21*a*, *b*) for $\psi_1^{(0)}$, $\psi_1^{(2)}$. Equation (5.10*b*) can be written as

$$\psi_{2yy}^{(1)} - d\bar{b}\psi_2^{(1)} = -(2C_{1Y}^{(0)} - \mathrm{i}\bar{\beta}_2 C_1^{(0)})R_1' - \bar{\alpha}_2\bar{\psi}_1, \tag{A 12}$$

whence we find $\psi_2^{(1)}$:

$$\psi_2^{(1)} = \frac{1}{2a}(2C_{1Y}^{(0)} - \mathrm{i}\bar{\beta}_2 C_1^{(0)})\varphi_2(y) - \bar{\alpha}_2\bar{\psi}_1 F_2(y) + C_1^{(1)}(Y)R_1. \tag{A 13}$$

Here $C_1^{(1)}(Y)$ is an arbitrary function, F_2 is a periodic function with period ω,

$$F_2 = -\frac{a\omega^2}{4\pi^2}\sum_{m,k}\frac{A_1^{(m)}A_1^{(k)}}{k^2}\mathrm{e}^{2\pi\mathrm{i}(m+k)y/\omega} + \frac{\omega}{2\pi\mathrm{i}}\sum_{m,n}\frac{(n-m)A_1^{(m)}A_2^{(n)}}{mn}\mathrm{e}^{2\pi\mathrm{i}(m+n)y/\omega}, \tag{A 14}$$

and $A_1^{(m)}$, $A_2^{(n)}$ are the coefficients in the Fourier series

$$\varphi_1(y) = \sum_m A_1^{(m)}\mathrm{e}^{2\pi\mathrm{i}my/\omega}, \quad \varphi_2(y) = \sum_n A_2^{(n)}\mathrm{e}^{2\pi\mathrm{i}ny/\omega}. \tag{A 15}$$

Requiring the orthogonality of the right-hand side of (5.11*b*) to R_1 and using (A 13) and the simple relation (following from (5.16) and (5.29)

$$\langle R_1\varphi_2'\rangle = \tfrac{1}{2}\left(1 - a\langle R_1^2\rangle\right) \tag{A 16}$$

we obtain the equation

$$C_{1YY}^{(0)} - \mathrm{i}\bar{\beta}_2 C_{1Y}^{(0)} - \left[\frac{\bar{\beta}_2^2}{4} + a\left(n_2 - \frac{\bar{\beta}_2^2}{4}\right)\langle R_1^2\rangle\right]C_1^{(0)} = -\bar{\alpha}_2 a\langle F_2 R_1'\rangle(2\bar{\psi}_{1Y} - \mathrm{i}\bar{\beta}_2\bar{\psi}_1) \tag{A 17}$$

relating the coefficient $C_1^{(0)}(Y)$ to the large-scale upper layer component $\bar{\psi}_1(Y)$.

In the case $A = 1$,

$$\langle R_1\rangle \neq 0 \tag{A 18}$$

we have from (A 10) and (5.10*a*)

$$\psi_{1YY}^{(0)} - \mathrm{i}\bar{\beta}_2\psi_{1Y}^{(0)} - n_1\psi_1^{(0)} = -\bar{\alpha}_1 C_1^{(0)}\langle R_1\rangle, \tag{A 19}$$

$$\psi_{1yy}^{(2)} = -\bar{\alpha}_1 C_1^{(0)}(R_1 - \langle R_1\rangle). \tag{A 20}$$

One can readily show that in (5.10*b*)

$$\langle K_1 R_1\rangle = -\bar{\alpha}_2\bar{\psi}_1\langle R_1\rangle \neq 0, \tag{A 21}$$

and, therefore, for $\psi_2^{(1)}$ to be bounded the lowest-order term $\bar{\psi}_1$ must vanish:

$$\bar{\psi}_1 = 0. \tag{A 22}$$

The solution to (5.10*b*) is given by the equation

$$\psi_2^{(1)} = \frac{1}{2a}(2C_{1Y}^{(0)} - \mathrm{i}\bar{\beta}_2 C_1^{(0)})\varphi_2(y) + C_1^{(1)}(Y)R_1. \tag{A 23}$$

Using (5.8*a*), (A 10), and (A 23) one can reduce the orthogonality of K_2 to R_1 in (5.11*b*) to the equation

$$C_{1YY}^{(0)} - \mathrm{i}\bar{\beta}_2 C_{1Y}^{(0)} - \left[\frac{\bar{\beta}_2^2}{4} + a\left(n_2 - \frac{\bar{\beta}_2^2}{4}\right)\langle R_1^2\rangle\right]C_1^{(0)} = -\bar{\alpha}_2\langle R_1\rangle\psi_1^{(0)}, \tag{A 24}$$

relating the coefficient $C_1^{(0)}(Y)$ to the lowest-order large-scale layer component $\psi_1^{(0)}(Y)$. The dispersion relation in this case follows from the existence of a solution to (A 19), (A 24) proportional to e^{ilY}. Obviously, the dispersion relation has nothing in common with the dispersion relation (5.17).

Appendix B

The investigation technique is based on the fact (e.g. Yakubovich & Starzhinsky 1972) that the vector equation

$$\frac{d\boldsymbol{x}}{dy} = \boldsymbol{A}(y)\boldsymbol{x}, \tag{B 1}$$

where

$$\boldsymbol{x} = \begin{pmatrix} \psi_1 \\ \vdots \\ \psi_n \end{pmatrix}$$

is an n-dimensional vector and $\boldsymbol{A}(y)$ a periodic $n \times n$ matrix with period ω, has a fundamental system of linearly independent solutions of the form

$$\boldsymbol{x}_\nu = e^{\alpha_\nu y}\boldsymbol{f}_\nu(y), \quad \nu = 1,\ldots,n. \tag{B 2}$$

Here $\alpha_\nu = 1/\omega \ln \rho_\nu$; ρ_ν, $\nu = 1,\ldots,n$, are the multiplicators of (B 1), which are the eigenvalues of the monodromy matrix. In turn, they can be found from the matrix equation for the $n \times n$ matrix $\boldsymbol{X}(y)$:

$$\frac{d\boldsymbol{X}}{dy} = \boldsymbol{A}(y)\boldsymbol{X} \tag{B 3}$$

with the 'initial' condition

$$\boldsymbol{X}(0) = \boldsymbol{I}_n, \tag{B 4}$$

where $\boldsymbol{I}_n$ is the $n \times n$ identity matrix. The monodromy matrix is equal to $\boldsymbol{X}(\omega)$. If the multiplicity of an eigenvalue ρ_{ν_0} is equal to 1, then the function $\boldsymbol{f}_{\nu_0}(y)$ in (B 2) is periodic with period ω. For ρ_{ν_0} with multiplicity $r > 1$ there exist r linearly independent functions $\boldsymbol{f}_{\nu_0}^{(k)}(y)$, $k = 1,\ldots,r$, one of which is periodic and the others have the form

$$\sum_{m=1}^{r} y^m \boldsymbol{g}_m(y),$$

where $\boldsymbol{g}_m(y)$ are periodic functions with period ω. The solutions (B 2) coincide at $y = 0$ with the eigenvectors $\boldsymbol{b}_\nu$ of the monodromy matrix, i.e.

$$\boldsymbol{x}_\nu(0) = \boldsymbol{b}_\nu. \tag{B 5}$$

If the modulus of a multiplicator ρ_{ν_0} is equal to unity and hence $\operatorname{Re}\alpha_{\nu_0} = 0$, then at least one bounded solution (B 2) corresponds to ρ_{ν_0}.

To analyse the eigenvalue problem (2.7*a*, *b*) we rewrite the system in the form (B 1) for the vector

$$\boldsymbol{x} = \begin{pmatrix} \psi_1 \\ \psi_2 \\ \psi_3 \\ \psi_4 \end{pmatrix}, \quad \psi_3 = \psi_1', \quad \psi_4 = \psi_2'. \tag{B 6}$$

For given k, σ, δ, and q we calculated on a computer the monodromy matrix using (B 3) and (B 4) and obtained the corresponding multiplicators ρ_ν. If at least one of these multiplicators ρ_ν, say, ρ_{ν_0} has a unit modulus, then at least one bounded solution (B 2) corresponds to ρ_{ν_0}, and therefore the given k, σ, δ, and q are the eigenvalues of the problem (2.7a, b). The corresponding eigenfunction $\boldsymbol{x}_{\nu_0}$ is found by solving (B 1) for the initial condition

$$\boldsymbol{x}_{\nu_0}(0) = \boldsymbol{b}_{\nu_0}. \tag{B 7}$$

If the multiplicity of ρ_{ν_0} is equal to 1, then the solution $\boldsymbol{x}_{\nu_0}$ is bounded for $-\infty < y < +\infty$. If the multiplicity of ρ_{ν_0} exceeds 1, then one should choose the eigenvector $\boldsymbol{b}_{\nu_0}$ corresponding to the periodic function $\boldsymbol{f}_{\nu_0}(y)$ in (B 2). Due to the periodicity of $\boldsymbol{f}_{\nu_0}(y)$ the function $\boldsymbol{x}_{\nu_0}(y)$ is completely determined by its behaviour on the interval $(0, \omega)$.

For $|\rho_{\nu_0}| = 1$ we have $\alpha_{\nu_0} = (\mathrm{i}/\omega)\arcsin(\operatorname{Im}\rho_{\nu_0})$, and therefore one can find the wavenumber $\bar{l}_{\nu_0}$ along y-axis by the formula

$$\bar{l}_{\nu_0} = \frac{1}{\omega}\arcsin(\operatorname{Im}\rho_{\nu_0}). \tag{B 8}$$

Knowing α_{ν_0} and $\boldsymbol{x}_{\nu_0}(y)$ we can determine the bounded solution in the form (6.3).

REFERENCES

Bobrovich, A. V. & Reznik, G. M. 1999 Planetary waves in a stratified ocean of variable depth. Part 2. Continuously stratified model. *J. Fluid Mech.* **388**, 147.

Chelton, D. B. & Shlax, M. G. 1996 Global observations of oceanic Rossby waves. *Science* **272**, 234.

Dickson, R. R. 1983 Global summaries and intercomparisons: flow statistics from long-term current meter moorings. In *Eddies in Marine Science* (ed. A. Robinson). Springer.

Kamenkovich, V. M., Koshlyakov, M. N. & Monin, A. S. 1986 *Synoptic Eddies in the Ocean.* Springer.

Kamenkovich, V. M. & Reznik, G. M. 1978 Rossby waves. In *Physics of the Ocean, Vol. 2. Hydrodynamics of the Ocean,* p. 300. Moscow, Nauka (in Russian).

McWilliams, J. C. 1974 Forced transient flow and small-scale topography. *Geophys. Astrophys. Fluid Dyn.* **6**, 49.

Pedlosky, J. 1979 *Geophysical Fluid Dynamics.* Springer.

Reznik, G. M. 1986 Rossby waves and synoptic variability of the ocean. *Doctoral Dissertation,* Moscow, IO RAS (in Russian).

Rhines, P. B. 1970 Edge-, bottom-, and Rossby waves in a rotating stratified fluid. *Geophys. Fluid Dyn.* **1**, 273.

Rhines, P. B. 1977 The dynamics of unsteady currents. In *The Sea, Vol. 6* (ed. E. Goldberg, I. McCane, J. O'Brien & J. Steele), pp. 189–318. Wiley.

Rhines, P. B. & Bretherton, F. 1973 Topographic Rossby waves in a rough-bottomed ocean. *J. Fluid Mech.* **61**, 583–607.

Samelson, R. M. 1992 Surface-intensified Rossby waves over rough topography. *J. Mar. Res.* **50**, 367.

Sengupta, D., Piterbarg, L. I. & Reznik, G. M. 1992 Localization of topographic Rossby waves over random relief. *Dyn. Atmos. Ocean.* **17**, 1.

Smirnov, V. I. 1974 *A Course of Higher Mathematics,* Vol. 3(2). Moscow, Nauka (in Russian).

Suarez, A. 1971 The propagation and geometry of topographic oscillations in the ocean. PhD thesis, Department of Meteorology, MIT.

Volosov, V. M. 1976*a* Nonlinear topographic Rossby waves. *Oceanology* **16** (3), 389 (in Russian).

Volosov, V. M. 1976*b* On the nonlinear theory of topographic Rossby waves. *Oceanology* **16** (5), 741 (in Russian).

Volosov, V. M. & Zhdanov, M. A. 1980*a* Linear theory of large-scale flows over an anizotropic bottom relief in a two-layer model of the ocean. *Oceanology* **20** (1), 5 (in Russian).

Volosov, V. M. & Zhdanov, M. A. 1980*b* Linear theory of large-scale flows over an anizotropic

bottom relief in a continuously stratified model of the ocean. *Oceanology* **20** (4), 581 (in Russian).

VOLOSOV, V. M. & ZHDANOV, M. A. 1982 Nonlinear theory of large-scale flows over an anizotropic bottom relief in a two-layer model of the ocean. *Oceanology* **22** (5), 698 (in Russian).

VOLOSOV, V. M. & ZHDANOV, M. A. 1983 Nonlinear theory of large-scale flows in a continuously stratified model of the ocean. *Oceanology* **23** (2), 204 (in Russian).

WUNSCH, C. 1981 Low-frequency variability of the sea. In *Evolution of Physical Oceanography. Scientific Surveys in Honor of Henry Stommel,* p. 342. MIT.

WUNSCH, C. 1983 Western Atlantic Interior. In *Eddies in Marine Science,* p. 46. Springer.

YAKUBOVICH, V. A. & STARZHINSKY, V. M. 1972 *Linear Differential Equations with Periodic Coefficients and their Applications.* Moscow, Nauka (in Russian).

ZHDANOV, M. A. 1987 On synoptic-scale motions in a two-layer ocean with uneven bottom. *Oceanology* **27** (3), 363 (in Russian).